Phys Chem Minerals (1998) 26:14–30

ORIGINAL PAPER

X. Xue · M. Kanzaki

Correlations between ^{29}Si, ^{17}O and ^{1}H NMR properties and local structures in silicates: an ab initio calculation

Received: 18 July 1997 / Revised, accepted: 23 February 1998

Abstract In order to gain insight into the correlations between ^{29}Si, ^{17}O and ^{1}H NMR properties (chemical shift and quadrupolar coupling parameters) and local structures in silicates, ab initio self-consistent field Hartree-Fock molecular orbital calculations have been carried out on silicate clusters of various polymerizations and intertetrahedral (Si-O-Si) angles. These include $Si(OH)_4$ monomers (isolated as well as interacting), $Si_2O(OH)_6$ dimers (C_2 symmetry) with the Si-O-Si angle fixed at 5° intervals from 120° to 180°, $Si_3O_2(OH)_8$ linear trimers (C_2 symmetry) with varying Si-O-Si angles, $Si_3O_3(OH)_6$ three-membered rings (D_3 and C_1 symmetries), $Si_4O_4(OH)_8$ four-membered ring (C_4 symmetry) and $Si_8O_{12}(OH)_8$ octamer (D_4 symmetry). The calculated ^{29}Si, ^{17}O and ^{1}H isotropic chemical shifts (δ_i^{Si}, δ_i^{O} and δ_i^{H}) for these clusters are all close to experimental NMR data for similar local structures in crystalline silicates. The calculated ^{17}O quadrupolar coupling constants (*QCC*) of the bridging oxygens (Si-O-Si) are also in good agreement with experimental data. The calculated ^{17}O *QCC* of silanols (Si-O-H) are much larger than those of the bridging oxygens, but unfortunately there are no experimental data for similar groups in well-characterized crystalline phases for comparison. There is a good correlation between δ_i^{Si} and the mean Si-O-Si angle for both Q^1 and Q^2, where Q^n denotes Si with n other tetrahedral Si next-nearest neighbors. Both the δ_i^{O} and the ^{17}O electric field gradient asymmetry parameter, η of the bridging oxygens have been found to depend strongly on the O site symmetry, in addition to the Si-O-Si angle. On the other hand, the ^{17}O *QCC* seems to be influenced little by structural parameters other than the Si-O-Si angle, and is thus expected to be the most reliable ^{17}O NMR parameter that can be used to decipher Si-O-Si angle distribution information. Both the ^{17}O *QCC* and the ^{2}H *QCC* of silanols decrease with decreasing length of hydrogen bond to a second O atom (Si-O-H···O), and the δ_i^{H} increase with the same parameter.

Key words ab initio · NMR · silicates · structure

X. Xue (✉) · M. Kanzaki
Institute for Study of the Earth's Interior, Okayama University, Misasa, Tottori, 682-0193 Japan
e-mail: xianyu@dbmac1.misasa.okayama-u.ac.jp

Introduction

Solid-state nuclear magnetic resonance spectroscopy (NMR) has proved to be a powerful tool in studying the local structure in silicates, because it is sensitive to the local electronic environment around a specific nucleus. In particular, Si and O, the dominant cation and anion in silicates, both have isotopes (^{29}Si and ^{17}O) amendable to NMR studies. Because ^{29}Si is a spin-1/2 nuclide with a reasonably high natural abundance (4.7%), a wealth of experimental ^{29}Si NMR data have been accumulated over the years, both for natural minerals and glasses and for synthetic silicates (see reviews in Engelhardt and Koller 1994; Stebbins 1995). The magic-angle spinning (MAS) NMR technique has commonly been utilized to obtain ^{29}Si isotropic chemical shifts. Correlations between ^{29}Si chemical shift and a number of structural parameters have been proposed, such as the coordination of Si, the tetrahedral polymerization, the Si-O bond length and the Si-O-Si angle (e.g., Smith and Blackwell 1983; Engelhardt and Radeglia 1984; Ramdas and Klinowski 1984; Janes and Oldfield 1985; Oestrike et al. 1987; Sherriff and Grundy 1988; Stebbins and Kanzaki 1991). Such correlations are useful in structural characterizations of disordered phases or crystalline phases with unknown structure.

There are much fewer ^{17}O NMR data available for silicate minerals and glasses. This is partly due to the low natural abundance of ^{17}O (0.037%), which limits its applicability mostly to isotopically enriched samples. In addition, being a quadrupolar nucleus of spin quantum number of 5/2, ^{17}O NMR peaks are often broadened by electric quadrupolar interactions between the nuclear electric quadrupole and the electric field gradient (*EFG*) at the nucleus. Such broadenings can only be partially removed by magic-angle spinning, rendering unique peak assignment

and quantification of MAS NMR spectra difficult, although the more sophisticated NMR techniques, such as dynamic-angle spinning (DAS) and double rotation (DOR) can effectively average out this second-order quadrupolar interaction, yielding narrow peaks for individual oxygen sites (see Chmelka and Zwanziger 1994 for a review). Nevertheless, the quadrupolar coupling of ^{17}O NMR is very sensitive to the local electronic environment at the oxygen nucleus and could thus be utilized for oxygen site identification under favorable conditions. The electric quadrupolar interaction of a quadrupolar nucleus, such as ^{17}O, can be described by two parameters: the quadrupolar coupling constant (*QCC*) that is proportional to the magnitude of the largest component of the *EFG* tensor at the nucleus, and the asymmetry parameter η (in the range $0 \sim 1$) that is a measure of the degree of deviation of the *EFG* tensor from axial symmetry. For crystalline silicates, these parameters may be obtained from simulations of static or MAS ^{17}O NMR spectra. It has been shown that a combination of the ^{17}O chemical shift and the *QCC* parameters can be used to distinguish bridging oxygens bonded to two different types of tetrahedral cations, (e.g., Si, Al or P), nonbridging oxygens (O atoms bonded to one tetrahedral cation) and oxygens bonded to three Si atoms (e.g., Timken et al. 1986a, b, 1987; Walter et al. 1988; Mueller et al. 1992; Xue et al. 1994). For amorphous silicates, it is difficult to distinguish peak broadenings from structural disorder and those from quadrupolar coupling. In this case, the more sophisticated techniques, such as DAS, DOR and multi-quantum MAS NMR, may be applied to extract these parameters. Farnan et al. (1992) has shown that the anisotropic dimension of two-dimensional ^{17}O DAS NMR spectra, due almost entirely to the electric quadrupolar coupling, may be simulated to yield distribution of quadrupolar parameters for an amorphous material. Similar information may also be gained, in principle, from two-dimensional multi-quantum MAS NMR. Such a distribution of quadrupolar parameters may be translated into the distribution of structural parameters, such as the Si-O-Si angle, when their correlations are unique (Farnan et al. 1992). The relationship between ^{17}O NMR parameters and the Si-O-Si angle is of particular interest, because, unlike Si, each bridging oxygen corresponds to only one Si-O-Si angle, and thus ^{17}O NMR may potentially yield more reliable information about the Si-O-Si angle distribution in amorphous silicates (see Farnan et al. 1992). Unfortunately, there have not been enough ^{17}O NMR data for crystalline silicates with well characterized structures to establish such correlations.

Another approach to study the correlations between NMR parameters and local structure is theoretical calculations. A widely used ab initio calculation method is self-consistent field Hartree-Fock molecular orbital calculation (SCF-HF MO) on small clusters that are constructed to model the local structural units in condensed phases. The discussion of Si-O-Si angle distribution from two-dimensional DAS spectra by Farnan et al. (1992) was mostly based on the result of this type of calculation by Tossell and Lazzeretti (1988) and Tossell (1990). Their calculations were, however, performed with relatively small basis sets (3–21G(d,p) or smaller basis sets), which yield unreliable chemical shifts. With the rapid advancement in computer technology, such calculations can now be improved to a large extent by employing much larger basis sets and/or incorporating electron correlations (beyond the HF approximation). We have shown in a previous study (Kanzaki 1996) that reliable ^{29}Si NMR chemical shift values can be obtained from SCF-HF MO calculations for $Si(OH)_4$, $Si(OH)_5^-$, $Si(OH)_6^{-2}$ clusters by using the more robust 6–311+G(2df,p) basis set, and by performing the calculations on tetramethylsilane (TMS, $Si(CH_3)_4$), the ^{29}Si chemical shift reference standard, in addition to the clusters of interest. We found that calculations with smaller basis sets, such as the 6–31G(d) basis set, yield unreliable chemical shift values. More recently, similar calculations on ^{29}Si, ^{27}Al and ^{1}H NMR properties have also been reported for silicate and aluminosilicate clusters of various polymerizations and sizes (Moravetski et al. 1996; Tossell and Sághi-Szabó 1997; Sykes et al. 1997).

The aim of the present study was to gain a better understanding of the correlations between ^{29}Si, ^{17}O and ^{1}H NMR properties and local structural parameters for silicates by performing SCF-HF MO calculations with the robust 6–311+G(2df,p) basis set for a number of silicate clusters that serve as models for SiO_4 tetrahedra in silicate minerals, glasses and solutions with different polymerizations and of varying intertetrahedral angles. These clusters include $Si(OH)_4$ monomers (isolated as well as interacting), $Si_2O(OH)_6$ dimers with the Si-O-Si angle fixed at 5° interval between 120° and 180°, $Si_3O_2(OH)_8$ linear trimers with varying Si-O-Si angles, $Si_3O_3(OH)_6$ three-membered rings, $Si_4O_4(OH)_8$ four-membered ring and $Si_8O_{12}(OH)_8$ octamer. Although the primary purpose of introducing H atoms into the clusters was for charge-balancing the dangling bonds on O at the peripheries of the clusters, SiOH (silanol) groups are often present on the surfaces and at structural defects of many silicates and in the interiors of hydrous silicates and silicate solutions. Our calculations should provide valuable insight into the ^{17}O and ^{1}H (^{2}H) NMR characteristics of such groups. In particular, the ^{17}O NMR characteristics of silanols have not been well documented from experimental NMR studies, although such information is very much needed in order to uniquely identify them in hydrous silicates and silicate solutions (e.g., Cong and Kirkpatrick 1993; Knight et al. 1989).

Calculation method

The calculations described in this study have been performed with the Gaussian 94 program (Frisch et al. 1995). In brief, we first carried out cluster geometry optimization using the restricted HF (RHF) method with the standard polarized split-valence 6–31G(d) basis set. The $Si(OH)_4$ monomer geometries (isolated as well as two- and three- freely interacting monomers) were optimized without any symmetry constraints. The resultant minimum-energy geometry

for the isolated monomer possesses S_4 point symmetry. For the $Si_2O(OH)_6$ dimer, optimization without any symmetry constraints led to a minimum-energy geometry with C_2 point symmetry. Geometry optimization for the $Si_2O(OH)_6$ dimer (C_2 symmetry) was also performed with the Si-O-Si angle fixed successively at 5° intervals between 120° and 180°. For the $Si_3O_2(OH)_8$ linear trimer, optimization was carried out with C_2 point symmetry, both without angle constraint and with fixed Si-O-Si angles of 145° and 160°. For the $Si_3O_3(OH)_6$ three-membered ring, optimizations with two types of symmetry constraints (C_1 and D_3 point symmetries) were carried out. The $Si_4O_4(OH)_8$ four-membered ring was optimized with C_4 point symmetry and the $Si_8O_{12}(OH)_8$ octamer optimized with D_4 point symmetry.

Geometries optimized at the RHF/6–31G(d) level were employed for subsequent magnetic shielding and *EFG* tensor calculations. The latter calculations have been performed using the RHF method with the robust triple split valence 6–311+G(2df,p) basis set. The continuous set of gauge transformation (CSGT) method (Keith and Bader 1993) has been adopted for the magnetic shielding tensor calculations. Electron correlations are neglected in this type of calculations.

In experimental NMR, chemical shift is normally reported relative to a reference standard material (liquid TMS for ^{29}Si and ^{1}H, and liquid H_2O for ^{17}O). To facilitate comparison with experimental data, we have also calculated magnetic shieldings for TMS (cluster with C_{3v} point symmetry) in an analogous way as for the silicate clusters of interest. The ^{29}Si and ^{1}H isotropic chemical shifts relative to TMS (δ_i^{Si} and δ_i^{H}) (in ppm) for a silicate cluster can then be calculated using the following equation:

$$\delta_i^{Si\,or\,H}(\text{cluster}) = \sigma_i^{Si\,or\,H}(\text{TMS}) - \sigma_i^{Si\,or\,H}(\text{cluster})$$

where σ_i is the ^{29}Si or ^{1}H isotropic magnetic shielding (in ppm) from the SCF-HF calculations. We have found previously (Kanzaki 1996) that the δ_i^{Si} for SiH_4 and SiF_4 clusters calculated with this procedure are within 4 ppm of the experimental values for the respective molecules (also see Table 1). To check further the reliability of such calculations, we have also calculated NMR properties for tetramethoxysilane (TMOS, $Si(OCH_3)_4$) cluster, the Si coordination of which (to four O atoms) resembles those of isolated tetrahedral Si in silicate minerals. The resultant δ_i^{Si} is within 3 ppm of the experimental value for this molecule (see Table 1). As shown in subsequent sections, the calculated δ_i^{Si} and δ_i^{H} for the silicate clusters described in this study are all close to the respective experimental NMR data for similar local structures in crystalline and amorphous silicates.

It should be pointed out that these small clusters are at best representative of isolated, rigid (without rotation/vibration) species in the gas phase, whereas most experimental NMR data are for condensed phases. The NMR chemical shifts of the latter would also be influenced by other factors, such as inter-molecular interactions (medium effect) and rotations/vibrations. Nevertheless the agreement (within ±4 ppm) between the calculated δ_i^{Si} for the small clusters and the corresponding experimental data for the same molecules (structural units) in condensed phases (liquids in the case of molecules, and solids in the case of silicate crystals and glasses) suggest that the effects on δ_i^{Si} from these other factors are probably insignificant.

For ^{17}O, we have performed analogous calculations for isolated H_2O molecules (which may be considered to be representative of gas-phase H_2O) (see Table 5). The ^{17}O isotropic chemical shift of a silicate cluster relative to the H_2O molecule (δ_i^{O}) (in ppm) may be calculated as the following:

$$\delta_i^{O}(\text{cluster}) = \sigma_i^{O}(H_2O\ \text{molecule}) - \sigma_i^{O}(\text{cluster})$$

where σ_i^{O} is the ^{17}O isotropic magnetic shielding (in ppm) from the SCF-HF calculations. In order to evaluate how well such calculations reproduce experimental ^{17}O NMR data, we have also made calculations for three other small molecules: H_3COCH_3 (methyl ether), $(CH_3)_3COC(CH_3)_3$ (*tert*-butyl ether) and $(CH_3)_3SiOSi(CH_3)_3$ (hexamethyl disiloxane). In these molecules, each O atom is bridged between two C or two Si atoms, the latter case is similar to those in silicate minerals and glasses. None of these clusters contain multiple bonds for which electron correlation contributions are known to be significant (see Cheeseman et al. 1996). The calculated δ_i^{O} (relative to isolated H_2O molecule) for these clusters are within ±15 ppm of the experimental values for the respective molecules in the liquid state (relative to liquid H_2O) (see Table 1). The calculated δ_i^{O} (relative to isolated H_2O molecule) for Si-O-Si linkages in the silicate clusters, as described subsequently, are 35.6∼52.8 ppm, also in good agreement with experimental ^{17}O NMR data for similar linkages in tectosilicates (40–52 ppm relative to liquid H_2O: see compilations in Stebbins 1995).

In the case of H_2O, it is well known from experimental NMR measurement (Florin and Alei 1967) that there is a large (36-ppm) gas-liquid shift in δ_i^{O}: oxygen is strongly deshielded in the liquid phase than in the gas phase due to strong hydrogen bonding (see ab initio calculations of Malkin et al. 1996). Because experimental ^{17}O NMR data are normally reported relative to liquid H_2O, the reasonable agreement (within ±15 ppm) between the calculated δ_i^{O} for the isolated clusters and the corresponding experimental data for condensed phases suggest that the gas-liquid shifts in δ_i^{O} for these systems are probably comparable to that of H_2O. The greater discrepancies (within ±15 ppm) between the calculated values and experimental data for δ_i^{O}, as compared to those for δ_i^{Si} (within ±4 ppm), may be a combined effect of greater variations in the gas-liquid δ_i^{O} shifts among different molecules and larger computation errors due to limited basis sets and/or negligence of electron correlations. The relative changes in δ_i^{O} among the silicate clusters themselves should be more reliable than the absolute δ_i^{O} values.

Unlike the shielding properties that depend strongly on the excited wave functions, the electric field gradient at the nucleus depends only on the groundstate wave functions. Thus even with the same

Table 1 Comparison of calculated and experimental ^{29}Si and ^{17}O chemical shifts (δ_i^{Si} and δ_i^{O}) for small molecules

Molecules	δ_i^{Si}			δ_i^{O}		
	Calculated[a]	Experimental[b]	Difference	Calculated[a]	Experimental	Difference
SiH_4	–88.1	–91.9	+3.8			
SiF_4	–112.2	–112.5	+0.3			
$Si(OCH_3)_4$ (TMOS)	–81.2	–78.5	–2.7	–24.7[c]		
H_3COCH_3				–40.0	–52.5	+12.5
$(CH_3)_3COC(CH_3)_3$ (tBuOtBu)				61.5	76.0	–14.5
$(CH_3)_3SiOSi(CH_3)_3$[d]	3.4	7.0	–3.6	31.4	43	–12

[a] Calculated δ_i^{Si} (δ_i^{O}) relative to isolated TMS (H_2O) molecule; magnetic shieldings are calculated at the RHF/6–311+G(2df,p) level

[b] Experimental δ_i^{Si} (δ_i^{O}) relative to TMS (H_2O) in the liquid state; experimental δ_i^{Si} and δ_i^{O} data for $(CH_3)_3SiOSi(CH_3)_3$ are from Olah et al. (1995) and Rühlmann et al. (1988), respectively, and those for the rest are compiled in Janes and Oldfield (1985) and Kintzinger (1982), respectively

[c] Average value of –23.3 (x2), –23.5 and –28.6 ppm

[d] Si-O-Si angle fixed at the experimental value of 148° (see Olah et al. 1995)

basis functions, the calculations are expected to give more reliable results for the electric field gradients than for the magnetic shieldings. The *EFG* tensor components are related to the NMR quadrupolar coupling parameters by the following equations:

$$QCC=e^2q_{zz}Q/h$$

$$\eta=(eq_{xx}-eq_{yy})/eq_{zz}$$

where eQ is the nuclear quadrupole moment of the nucleus of interest; eq_{xx}, eq_{yy} and eq_{zz} are the components of the *EFG* tensor at the nucleus in the principle axis system, with $|eq_{zz}|\geq|eq_{yy}|\geq|eq_{xx}|$. Because the nuclear quadrupole moment eQ cannot be measured experimentally, it has normally been derived from the experimental *QCC* value and the calculated *EFG* for free atom (ground state atomic O ($^3P_2$) in the case of ^{17}O). The resultant eQ value is thus dependent on the method and basis sets of the *EFG* calculation. For ^{17}O, an eQ value of –0.0263 barns (1 barn=10^{-28} m^2) has been derived from *EFG* calculation for atomic O with the configuration interaction (CI)-HF method (Kelly 1969); whereas a value of –0.02233 barns, adopted by Tossell and Lazzeretti (1988) and Tossell (1990), has been reported from RHF calculations (Schaefer et al. 1968). In order to achieve internal consistency and better agreement with experimental data, it is best to use an eQ value calculated at the same level as for the studied clusters. From such a consideration, we have used, for ^{17}O *QCC* calculations, an eQ value (–0.02426 barns) derived from the accurate experimental ^{17}O *QCC* value for H_2O molecule (10.175±0.067 MHz: Verhoeven et al. 1969) and the ^{17}O *EFG* value (eq_{zz}=–1.785034 a.u.) for the same molecule calculated in the same way as for the silicate clusters. The calculated ^{17}O *EFG* asymmetry parameter η for H_2O is 0.84, within 12% of the experimental value (0.75±0.01: Verhoeven et al. 1969). The ^{17}O *QCC* values for silicate clusters calculated in this way quantitatively agree with experimental NMR data (see details later). All the calculated silicate clusters have negative ^{17}O *QCC* values, and only the absolute values will be discussed in the text because experimental NMR do not often distinguish the sign of the *QCC*.

For ^2H, we have adopted an eQ value of +0.002444 barns derived from the experimental ^2H *QCC* value for ^2H_2O molecule (307.95±0.14 kHz: Verhoeven et al. 1969) and the calculated ^2H *EFG* value for the same molecule (eq_{zz}=0.536189 a.u.). The calculated ^2H EFG asymmetry parameter η for ^2H_2O is 0.1228, within 9% of the experimental value (0.1350±0.0007: Verhoeven et al. 1969).

Results and Discussion

Optimized geometries

Selected structural parameters for the $Si(OH)_4$ monomer, $Si_2O(OH)_6$ dimers, $Si_3O_2(OH)_8$ linear trimers, $Si_3O_3(OH)_6$ three-membered rings, $Si_4O_4(OH)_8$ four-membered ring and $Si_8O_{12}(OH)_8$ octamer are compiled in Tables 2–5. One structural aspect of these clusters that affects the ^{17}O and ^1H (^2H) NMR properties of silanols is hydrogen bonding. As described later, H···O bridging bonds with distances greater than about 2.6 Å do not exhibit significant effect on such properties (see Figs. 8,9). Therefore, only those H···O pairs that are separated by ≤2.6 Å are identified as hydrogen bonds from the perspective of NMR properties.

The optimized geometry for $Si(OH)_4$ monomer with S_4 point symmetry has been reported in a previous paper (Kanzaki 1996) (see also Table 2). Each H atom is at a distance of 2.70 Å from a neighboring O atom.

The optimized structure of the $Si_2O(OH)_6$ dimers with C_2 point symmetry (see Fig. 1 and Table 2) has a Si-O_{br} (bridging oxygen, also BO) bond length of 1.623 Å and a Si-O-Si angle of 131.72°, in agreement with the calcu-

Table 2 Geometry parameters and energies for $Si(OH)_4$ monomer, $Si_2O(OH)_6$ dimers, $Si_3O_2(OH)_8$ linear trimers, $Si_3O_3(OH)_6$ three-membered rings, $Si_4O_4(OH)_8$ four-membered ring and $Si_8O_{12}(OH)_8$ octamer calculated at the RHF/6–31G(d) level

Cluster	∠Si-O-Si[a] (°)	R(Si-O_{br})[a] (Å)	R(Si-OH)[a] (Å)	∠O-Si-O[a] (°)	Energy (hartree)[b]
Monomer (S_4)	–	–	1.629	106.39, 115.83 (109.54)	–590.89169 (–591.07461)
Dimer (C_2)	120	1.637	(1.629)	103.77–113.36 (109.49)	–1105.77921 (–1106.09747)
Dimer (C_2)	125	1.630	(1.629)	103.54–113.51 (109.49)	–1105.78094 (–1106.09998)
Dimer (C_2)	130	1.625	(1.629)	103.57–113.73 (109.49)	–1105.78155 (–1106.10134)
Dimer (C_2)	131.72[c]	1.623	(1.629)	103.65–113.75 (109.49)	–1105.78159 (–1106.10160)
Dimer (C_2)	135	1.621	(1.629)	103.78–113.77 (109.50)	–1105.78150 (–1106.10194)
Dimer (C_2)	140	1.618	(1.628)	104.09–113.92 (109.50)	–1105.78111 (–1106.10210)
Dimer (C_2)	145	1.615	(1.628)	104.42–114.04 (109.50)	–1105.78059 (–1106.10201)
Dimer (C_2)	150	1.613	(1.628)	104.74–114.13 (109.50)	–1105.78004 (–1106.10181)
Dimer (C_2)	155	1.612	(1.628)	104.95–114.18 (109.50)	–1105.77951 (–1106.10155)
Dimer (C_2)	160	1.610	(1.628)	105.14–114.22 (109.50)	–1105.77904 (–1106.10129)
Dimer (C_2)	165	1.609	(1.628)	105.28–114.23 (109.51)	–1105.77864 (–1106.10104)
Dimer (C_2)	170	1.608	(1.628)	105.37–114.25 (109.51)	–1105.77831 (–1106.10079)
Dimer (C_2)	175	1.607	(1.628)	105.43–114.24 (109.51)	–1105.77806 (–1106.10061)
Dimer (C_2)	180	1.607	(1.628)	105.46–114.24 (109.51)	–1105.77787 (–1106.10046)
Trimer (C_2)	131.70[c]	1.614, 1.627 (1.620)	(1.630)	103.63–113.71 (109.50)	–1620.67093 (–1621.12864)
Trimer (C_2)	145	1.606, 1.624 (1.615)	(1.629)	104.53–114.60 (109.37)	–1620.66986 (–1621.12962)
Trimer (C_2)	160	1.603, 1.614 (1.609)	(1.629)	104.99–114.45 (109.50)	–1620.66655 (–1621.12815)
3-ring (D_3)	132.32	1.626	1.625	106.69–111.92 (109.47)	–1544.64440 (–1545.06296)
3-ring (C_1)	(133.48)	1.626–1.633 (1.630)	(1.622)	105.39–114.03 (109.49)	–1544.64756 (–1545.06572)
4-ring (C_4)	137.19	1.625, 1.627 (1.626)	(1.625)	106.47–113.34 (109.47)	–2059.54457 (–2060.09614)
Octamer (D_4)	(149.32)	1.615–1.621 (1.618)	1.615	107.89–111.35 (109.47)	–3815.05090 (–3815.99405)

[a] Data in brackets are the average values
[b] 1 hartree=4.3597×10^{-18} J; energy values in bracket are those calculated at the RHF/6–311+G(2df,p) level
[c] Optimum Si-O-Si angle at the RHF/6–31G(d) level

Table 3 ^{29}Si magnetic shielding and chemical shift parameters for TMS ($Si(CH_3)_4$), TMOS ($Si(OCH_3)_4$), $Si(OH)_4$ monomers, $Si_2O(OH)_6$ dimers, $Si_3O_2(OH)_8$ trimers, $Si_3O_3(OH)_6$, $Si_4O_4(OH)_8$ rings and $Si_8O_{12}(OH)_8$ octamer calculated at the RHF/6–311+G(2df,p) level

Cluster	∠Si-O-Si (°)[a]	σ_i^{Si} ppm	$\Delta\sigma^{Si}$ ppm	η^{Si}	δ_i^{Si} ppm
TMS	–	385.52	0.006	0.03	0.00
TMOS	–	466.76	21.46	0.65	–81.24
Monomer	–	457.19	16.24	0.00	–71.67
2monomerSi1	–	456.64	–30.18	0.21	–71.11
Si2	–	456.61	26.22	0.41	–71.09
3monomerSi1	–	458.37	15.82	1.00	–72.85
Si2	–	455.96	28.60	0.80	–70.44
Si3	–	457.80	–21.07	0.90	–72.28
Dimer	120	459.24	21.94	0.41	–73.72
Dimer	125	460.82	22.29	0.24	–75.30
Dimer	130	462.29	21.99	0.10	–76.77
Dimer	131.72	462.75	21.70	0.07	–77.23
Dimer	135	463.60	21.27	0.05	–78.08
Dimer	140	464.80	20.37	0.16	–79.28
Dimer	145	465.87	19.51	0.27	–80.35
Dimer	150	466.85	18.82	0.37	–81.33
Dimer	155	467.71	18.30	0.47	–82.19
Dimer	160	468.46	17.86	0.55	–82.94
Dimer	165	469.07	17.66	0.62	–83.55
Dimer	170	469.50	17.39	0.67	–83.98
Dimer	175	469.76	17.33	0.72	–84.24
Dimer	180	469.83	17.25	0.75	–84.30
Trimer, Q^1	131.70	462.71	22.54	0.19	–77.19
Q^2	131.70	468.34	–14.22	0.68	–82.82
Trimer, Q^1	145	465.67	21.99	0.78	–80.15
Q^2	145	475.84	–9.25	0.01	–90.32
Trimer, Q^1	160	468.41	21.35	0.66	–82.89
Q^2	160	480.47	–6.93	0.28	–94.95
3-ring (D_3)	132.32	469.43	–25.00	0.83	–83.91
3-ring (C_1), Si1	133.60, 134.02 (133.81)	470.33	29.79	0.71	–84.81
Si2	132.82, 133.60 (133.21)	470.30	30.97	0.84	–84.78
Si3	132.82, 134.02 (133.42)	470.11	32.68	0.70	–84.59
4-ring	137.19	471.23	37.28	0.64	–85.70
Octamer	147.05, 150.46 (×2) (149.32)	486.96	39.93	0.30	–101.44

Note: σ_i^{Si} is the ^{29}Si isotropic magnetic shielding; shielding anisotropy ($\Delta\sigma^{Si}$)=σ_{33}–(σ_{11}+σ_{22})/2, where σ_{11}, σ_{22}, σ_{33} are the components of the ^{29}Si magnetic shielding tensor with $|\sigma_{33}-\sigma_i|\geq|\sigma_{11}-\sigma_i|\geq|\sigma_{22}-\sigma_i|$; Note that chemical shift anisotropy ($\Delta\delta^{Si}$) has opposite sign; shielding asymmetry (η^{Si})=(σ_{22}–σ_{11})/(σ_{33}–σ_i); isotropic chemical shift (δ_i^{Si}) relative to TMS

[a] Data in brackets are average values

lations by Xiao and Lasaga (1994). Single-point energy calculations suggest that the Si-O-Si angle of the optimized structure becomes larger (around 140°) at the RHF/6–311+G(2df,p) level (see Table 2). The Si-OH bond lengths range from 1.621 Å to 1.637 Å with a somewhat larger average value (1.629 Å) than the Si-O_{br} bond length. The O-Si-O angles of the SiO_4 tetrahedra vary from 103.65° to 113.75°, with an average value of 109.49°. The O-H bond lengths are 0.947 Å (x4) and 0.950 Å (x2), with an average value of 0.948 Å (Table 5). Two of the H atoms (in the Si-O-Si bending direction) each form an O···H bridging bond with a silanol oxygen from a different SiO_4 tetrahedron at a distance of 2.51 Å (see Fig. 1). The distances for all the other O···H pairs are ≥2.72 Å. For the $Si_2O(OH)_6$ dimers optimized with a fixed Si-O-Si angle, the Si-O_{br} bond length decreases with increasing Si-O-Si angle from 1.637 Å at 120° to 1.607 Å at 180°, whereas the average Si-OH bond length varies only slightly (see Fig. 2 and Table 2). The length of the two O···H bridging bonds increases rapidly with increasing Si-O-Si angle from 2.25 Å at 120° to ≥2.61 Å above 135°.

The optimized geometry for the $Si_2O(OH)_6$ linear trimer with C_2 symmetry (see Fig. 1) has two equal Si-O-Si angles of 131.70°, close to that of the optimized $Si_2O(OH)_6$ dimer. As with the $Si_2O(OH)_6$ dimer, the Si-O-Si angles of the optimized $Si_2O(OH)_6$ linear trimer structure seem to be larger at the RHF/6–311+G(2df,p) level (see Table 2). The two identical bridging oxygen atoms are each bonded to two Si with uneven Si-O_{br} bond lengths of 1.614 Å (to central Si) and 1.627 Å (see Figs. 1, 2 and Table 2). The average Si-O_{br} bond length (1.620 Å) is slightly shorter than that of the optimized $Si_2O(OH)_6$ dimer. The Si-OH bond lengths range from 1.620 to 1.637 Å with a somewhat larger average value (1.630 Å) than the average Si-O_{br} bond length (Table 2). The O-H bond lengths range between 0.947–0.950 Å with an average value of 0.949 Å (Table 5). Two of the H atoms from the end SiO_4 tetrahedra (in the Si-O-Si bending directions) each form an O···H bridging bond with a sil-

Table 4 ^{17}O NMR shielding and *EFG* parameters for bridging oxygens (Si-O-Si) in the $Si_2O(OH)_6$ dimers, $Si_3O_2(OH)_8$ trimers, $Si_3O_3(OH)_6$ three-membered rings, $Si_4O_4(OH)_8$ four-membered ring and $Si_8O_{12}(OH)_8$ octamer calculated at the RHF/6–311+G(2df,p) level

Cluster	∠Si-O-Si	^{17}O shielding parameters				^{17}O EFG parameters		
	(°)	σ_i^O (ppm)	$\Delta\sigma^O$ (ppm)	η^O	δ_i^O (ppm)	eq_{zz}^O (a.u.)	$-QCC$[a] (MHz)	η
Dimer	120	268.66	42.28	0.43	50.11	0.783	4.46	0.75
Dimer	125	271.40	46.76	0.32	47.37	0.828	4.72	0.60
Dimer	130	273.70	51.40	0.22	45.07	0.865	4.93	0.49
Dimer	131.72	274.36	52.94	0.19	44.40	0.875	4.99	0.46
Dimer	135	275.74	56.21	0.14	43.03	0.895	5.10	0.40
Dimer	140	277.47	60.45	0.07	41.30	0.920	5.24	0.34
Dimer	145	278.94	64.35	0.03	39.83	0.942	5.37	0.28
Dimer	150	280.19	67.75	0.00	38.58	0.961	5.48	0.24
Dimer	155	281.24	70.72	0.02	37.53	0.977	5.57	0.20
Dimer	160	281.99	72.95	0.03	36.78	0.990	5.64	0.17
Dimer	165	282.59	74.80	0.04	36.18	0.999	5.70	0.14
Dimer	170	282.97	76.06	0.04	35.80	1.006	5.74	0.13
Dimer	175	283.18	76.92	0.04	35.59	1.010	5.75	0.12
Dimer	180	283.20	77.28	0.04	35.56	1.010	5.76	0.11
Trimer	131.70	276.80	53.32	0.28	41.97	0.882	5.03	0.46
Trimer	145	280.32	64.10	0.06	38.45	0.946	5.39	0.17
Trimer	160	283.00	73.05	0.02	35.76	0.995	5.67	0.12
3-ring (D_3)	132.32	276.37	43.40	0.04	42.39	0.895	5.10	0.29
3-ring (C_1) O1	133.60	269.24	39.77	0.13	49.53	0.889	5.07	0.10
O2	132.82	268.06	40.05	0.10	50.71	0.881	5.02	0.20
O3	134.02	268.47	38.93	0.16	50.29	0.889	5.07	0.11
4-ring	137.19	268.99	55.43	0.32	49.78	0.898	5.12	0.22
Octamer O1	147.05	266.02	61.27	0.16	52.75	0.959	5.47	0.21
O2	150.46	272.80	61.82	0.28	45.97	0.972	5.54	0.23

Note: σ_i^O is the ^{17}O isotropic magnetic shielding; shielding anisotropy ($\Delta\sigma^O$)=σ_{33}–(σ_{11}+σ_{22})/2, where σ_{11}, σ_{22}, σ_{33} are the components of the ^{17}O magnetic shielding tensor with $|\sigma_{33}-\sigma_i|\geq|\sigma_{11}-\sigma_i|\geq|\sigma_{22}-\sigma_i|$; (note that the chemical shift anisotropy $\Delta\delta^O$ has opposite sign); shielding asymmetry (η^O)=(σ_{22}–σ_{11})/(σ_{33}–σ_i) (note the difference between the shielding asymmetry η^O and the EFG asymmetry η parameters); isotropic chemical shift (δ_i^O) relative to H_2O

[a] All *QCC* values normalized to the experimental value of H_2O

anol oxygen from the central SiO_4 tetrahedron at a distance of 2.49 Å (see Fig. 1). The length of such O···H bridging bonds becomes shorter (2.40 Å) in the geometry with Si-O-Si angles of 145°, but is longer (2.84 Å) in the geometry with Si-O-Si angles of 160°. The distances for all the other O···H pairs are ≥2.70 Å.

In the optimized geometry for the $Si_3O_3(OH)_6$ three-membered ring with D_3 point symmetry, the three SiO_4 tetrahedra form a planner three-membered ring with even Si-O-Si angles of 132.32° (see Fig. 1). All the Si-O_{br} bond lengths are 1.626 Å, slightly longer than that of the $Si_2O(OH)_6$ dimer with the same Si-O-Si angle (see Fig. 2). The Si-OH bond lengths are 1.625 Å, similar to the Si-O_{br} bond lengths. The O-H bond lengths are 0.947 Å. All the O···H distances are ≥2.95 Å, lacking effective hydrogen bonds.

The optimized geometry for the $Si_3O_3(OH)_6$ three-membered rings with C_1 symmetry has a slightly lower energy than the one with D_3 symmetry described (see Table 2). In this structure, the three SiO_4 tetrahedra form a puckered three-membered ring, similar to that of Kubicki and Sykes (1993) calculated with the smaller 3–21G(d) basis set. There are three uneven Si-O-Si angles of 132.82°, 133.60°, and 134.02° with an average value of 133.48°, slightly larger that of the structure optimized with D_3 symmetry (Tables 2, 4). The Si-O_{br} bond lengths range from 1.626 to 1.633 Å with an average value of 1.630 Å, somewhat larger than that of the structure with D_3 symmetry (Table 2, Fig. 2). The lengths of the six Si-OH bonds range from 1.618 to 1.626 Å, with an average value of 1.622 Å, slightly shorter than the average Si-O_{br} bond length (Table 2). All the O-H bond lengths are around 0.947 Å (Table 5). The distances for all the O···H pairs are ≥2.72 Å, again lacking effective hydrogen bonds.

In the optimized geometry for the $Si_4O_4(OH)_8$ four-membered ring with C_4 symmetry, the four SiO_4 tetrahedra form a puckered four-membered ring with even Si-O-Si angles of 137.19°, an average Si-O_{br} bond length of 1.626 Å, a similar average Si-OH bond length of 1.625 Å, and an average O-H bond length of 0.949 Å (see Figs. 1, 2 and Tables 2,5). Like the three-membered rings, the average Si-O_{br} bond length is somewhat longer than that of the $Si_2O(OH)_6$ dimer with the same Si-O-Si angle (see Fig. 2). The four hydroxyls (OH) in the Si-O-Si bending directions each form two hydrogen bonds with a H and an O atom from two neighboring hydroxyls at a distance of 2.40 Å (see Fig. 1). The distances for all the other O···H pairs are ≥2.66 Å.

In the case of the optimized geometry for the $Si_8O_{12}(OH)_8$ octamer (double four-membered rings) with D_4 symmetry, each face of the cubic octamer consists of a puckered four-membered ring with Si-O-Si angles of 150.46° or 147.05°. The Si-O_{br} bond lengths range from

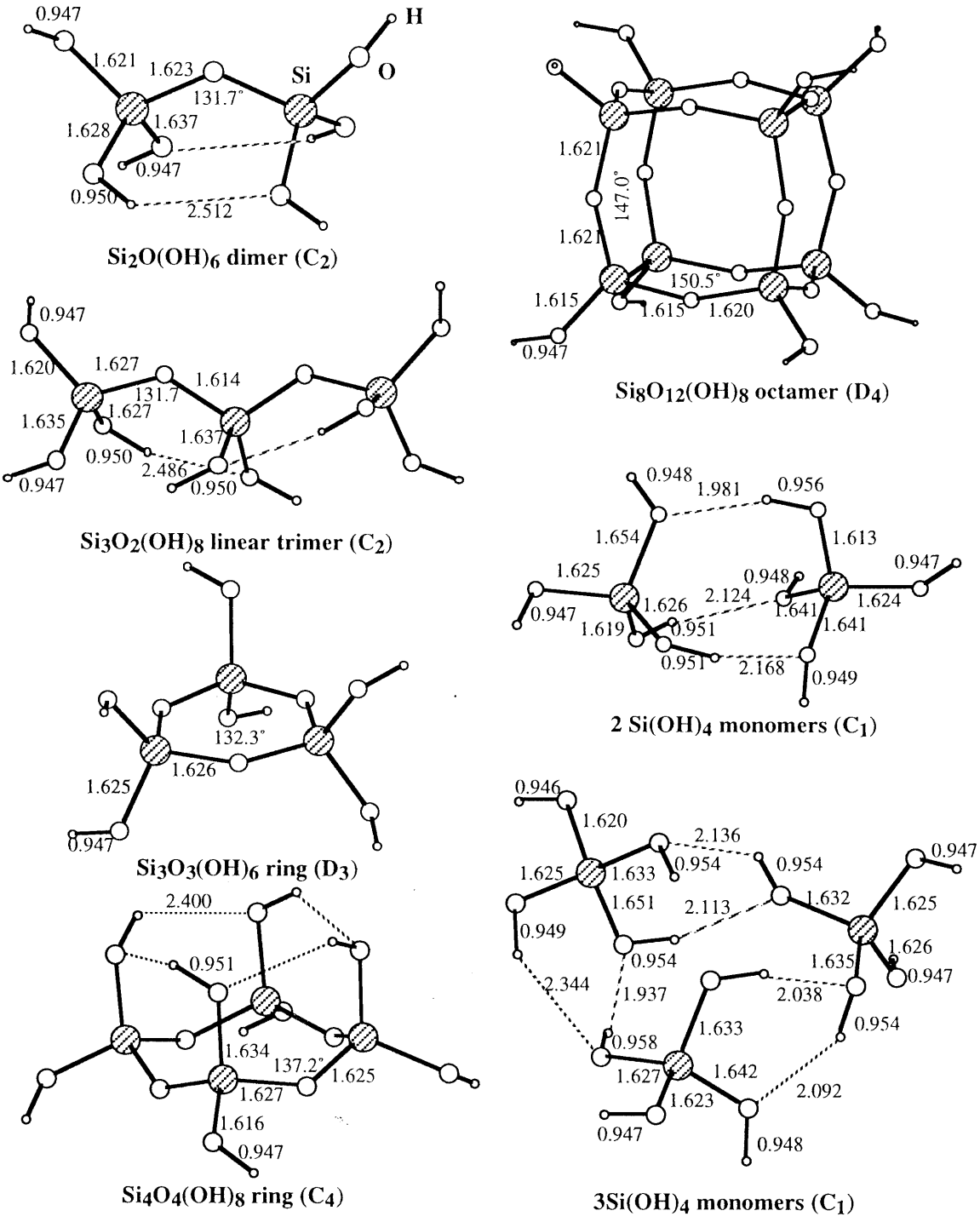

Fig. 1 Optimized geometries of $Si_2O(OH)_6$ dimer (C_2 symmetry), $Si_3O_2(OH)_8$ linear trimer (C_2 symmetry), $Si_3O_3(OH)_6$ three-membered ring (D_3 symmetry), $Si_4O_4(OH)_8$ four-membered ring (C_4 symmetry), $Si_8O_{12}(OH)_8$ octamer (D_4 symmetry), as well as two- and three- interacting $Si(OH)_4$ monomers. *Numbers* on the figures indicate values of the bond length (Å) and bond angle (°). *Broken lines* denote hydrogen bonds with H···O distances ≤2.6 Å

1.615 Å to 1.621 Å, with an average value of 1.619 Å, longer than that of the $Si_2O(OH)_6$ dimer with the same Si-O-Si angle (see Fig. 2). The Si-OH bond lengths are slightly shorter (1.615 Å), and the O-H bond lengths are 0.947 Å (see Figs. 1, 2 and Tables 2, 5). There are no significant hydrogen bonding, with the distances for all the O···H pairs ≥2.84 Å.

On the surfaces and in the interiors of hydrous silicates, silanols often interact with each other through hydrogen bonding (see Sauer et al. 1994), whereas for the isolated clusters described, the intramolecular hydrogen

Table 5 ^{17}O and ^{1}H (^{2}H) NMR parameters for TMS ($Si(CH_3)_4$), H_2O and silanols (SiOH) in the $Si(OH)_4$ monomers, $Si_2O(OH)_6$ dimers, $Si_3O_2(OH)_8$ trimers, $Si_3O_3(OH)_6$ three-membered rings, $Si_4O_4(OH)_8$ four-membered ring and $Si_8O_{12}(OH)_8$ octamer calculated at the RHF/6–311+G(2df,p) level

Cluster[a]	R(O-H)	R(H…O)	R(O…O)	^{17}O parameters[b]				^{1}H and ^{2}H parameters[c]			
	(Å)	(Å)	(Å)	σ_i^O (ppm)	δ_i^O (ppm)	eq_{zz}^O (a.u.)	$\|QCC\|^O$ (MHz)	σ_i^H (ppm)	δ_i^H (ppm)	eq_{zz}^H (a.u.)	QCC^H (kHz)
TMS								32.01	0.00	0.3291	189.0
H_2O	0.9474			318.77	0.00	–1.785	10.175	30.97	1.04	0.5362	307.95
Monomer	0.9469			301.73	17.04	1.42	8.09	30.31	1.71	0.5345	307.0
Dimer, 120	0.9470			304.52	14.25	1.42	8.11	30.22	1.79	0.5336	306.5
	0.9510	2.25	2.96	294.55	24.21	1.34	7.61	29.08	2.93	0.5047	289.9
	0.9475			297.11	21.66	1.41	8.05	30.25	1.76	0.5313	305.2
Dimer, 125	0.9470			304.44	14.33	1.42	8.11	30.21	1.80	0.5334	306.4
	0.9509	2.34	3.06	295.72	23.05	1.35	7.72	29.27	2.75	0.5072	291.3
	0.9473			298.33	20.43	1.41	8.03	30.29	1.72	0.5323	305.7
Dimer, 130	0.9470			304.23	14.53	1.42	8.10	30.21	1.80	0.5335	306.4
	0.9505	2.47	3.17	296.55	22.22	1.37	7.82	29.47	2.55	0.5111	293.6
	0.9472			299.40	19.36	1.41	8.03	30.32	1.69	0.5332	306.2
Dimer, 131.72	0.9471			304.15	14.61	1.42	8.10	30.21	1.80	0.5332	306.2
	0.9503	2.51	3.22	296.76	22.01	1.38	7.86	29.53	2.48	0.5126	294.4
	0.9471			299.72	19.05	1.41	8.03	30.33	1.68	0.5334	306.4
Dimer, 135	0.9470			303.99	14.78	1.42	8.11	30.22	1.79	0.5335	306.4
	0.9499	2.61	3.31	297.09	21.68	1.39	7.91	29.66	2.36	0.5156	296.1
	0.9470			300.14	18.63	1.41	8.04	30.35	1.66	0.5338	306.6
Dimer, 140	0.9470			303.69	15.08	1.42	8.11	30.23	1.78	0.5338	306.6
	0.9494			297.39	21.38	1.40	7.98	29.80	2.21	0.5194	298.3
	0.9469			300.75	18.01	1.41	8.05	30.37	1.64	0.5343	306.9
Dimer, 145	0.9470			303.45	15.32	1.42	8.11	30.24	1.77	0.5339	306.6
	0.9489			297.55	21.21	1.41	8.02	29.92	2.09	0.5227	300.2
	0.9469			301.10	17.66	1.41	8.06	30.39	1.62	0.5346	307.1
Dimer, 150	0.9470			303.22	15.55	1.42	8.11	30.25	1.76	0.5340	306.7
	0.9485			297.64	21.13	1.41	8.06	30.02	2.00	0.5253	301.7
	0.9468			301.31	17.46	1.42	8.07	30.40	1.61	0.5349	307.2
Dimer, 155	0.9470			302.93	15.83	1.42	8.11	30.26	1.75	0.5341	306.7
	0.9481			297.73	21.03	1.42	8.08	30.09	1.92	0.5274	302.9
	0.9468			301.39	17.38	1.42	8.08	30.42	1.60	0.5350	307.3
Dimer, 160	0.9469			302.82	15.95	1.42	8.12	30.27	1.75	0.5342	306.8
	0.9479			297.75	21.02	1.42	8.10	30.15	1.87	0.5290	303.8
	0.9468			301.45	17.32	1.42	8.09	30.43	1.59	0.5352	307.4
Dimer, 165	0.9469			302.62	16.15	1.42	8.12	30.27	1.74	0.5343	306.9
	0.9477			297.75	21.01	1.42	8.11	30.19	1.82	0.5302	304.5
	0.9468			301.48	17.29	1.42	8.10	30.43	1.58	0.5354	307.5
Dimer, 170	0.9470			302.49	16.27	1.42	8.12	30.27	1.74	0.5341	306.7
	0.9475			297.80	20.96	1.42	8.12	30.22	1.79	0.5312	305.1
	0.9468			301.42	17.35	1.42	8.10	30.44	1.57	0.5355	307.5
Dimer, 175	0.9469			302.39	16.38	1.42	8.12	30.28	1.74	0.5343	306.9
	0.9474			297.78	20.99	1.43	8.13	30.25	1.76	0.5320	305.6
	0.9468			301.45	17.32	1.42	8.11	30.45	1.56	0.5356	307.6
Dimer, 180	0.9470			302.31	16.45	1.42	8.12	30.28	1.74	0.5342	306.8
	0.9473			297.75	21.02	1.43	8.13	30.26	1.75	0.5326	305.9
	0.9468			301.44	17.32	1.42	8.12	30.45	1.56	0.5357	307.7
Trimer, 131.70[d]	0.9471			304.51	14.26	1.42	8.11	30.20	1.81	0.5332	306.3
	0.9471			300.05	22.81	1.41	8.04	30.37	1.65	0.5335	296.7
	0.9505	2.49	3.19	296.60	18.71	1.37	7.84	29.48	2.53	0.5114	306.4
	0.9499			295.96	22.17	1.38	7.87	29.69	2.32	0.5167	293.7
Trimer, 145[d]	0.9470			302.58	16.19	1.42	8.11	30.27	1.74	0.5338	306.6
	0.9468			301.50	17.26	1.42	8.11	30.42	1.60	0.5354	307.5
	0.9501	2.40	3.14	297.43	21.34	1.38	7.84	29.45	2.56	0.5114	293.7
	0.9478			297.44	21.32	1.41	8.02	30.15	1.86	0.5291	303.9
Trimer, 160[d]	0.9470			302.24	16.53	1.42	8.12	30.27	1.74	0.5339	306.7
	0.9467			301.76	20.43	1.41	8.01	30.42	1.59	0.5357	305.7
	0.9483			297.88	17.01	1.42	8.07	30.02	1.99	0.5256	307.7
	0.9473			298.33	20.89	1.42	8.09	30.31	1.70	0.5323	301.9

Table 5 (continued)

Cluster[a]	R(O-H)	R(H…O)	R(O…O)	^{17}O parameters[b]				^{1}H and ^{2}H parameters[c]			
	(Å)	(Å)	(Å)	σ_i^O (ppm)	δ_i^O (ppm)	eq_{zz}^O (a.u.)	$\|QCC\|^O$ (MHz)	σ_i^H (ppm)	δ_i^H (ppm)	eq_{zz}^H (a.u.)	QCC^H (kHz)
3-ring (D_3)	0.9469			297.41	21.36	1.44	8.21	30.39	1.62	0.5357	307.7
3-ring (C_1)	0.9471			300.26	18.51	1.43	8.14	30.18	1.83	0.5324	305.8
	0.9468			304.05	14.72	1.43	8.13	30.27	1.74	0.5341	306.7
	0.9467			303.11	15.66	1.43	8.13	30.29	1.72	0.5349	307.2
	0.9466			300.08	18.69	1.44	8.19	30.33	1.69	0.5358	307.8
	0.9466			303.03	15.74	1.43	8.16	30.23	1.78	0.5348	307.2
	0.9471			299.38	19.39	1.43	8.18	30.27	1.74	0.5331	306.2
4-ring	0.9467			304.16	14.61	1.45	8.25	30.07	1.94	0.5337	306.5
	0.9505	2.40	3.10	294.34	24.42	1.37	7.83	29.25	2.77	0.5078	291.6
Octamer	0.9467			304.89	13.88	1.45	8.25	30.31	1.70	0.5352	307.4
2monomer	0.9469			306.66	12.10	1.43	8.13	30.24	1.77	0.5344	306.9
	0.9483			296.83	21.94	1.42	8.08	30.15	1.86	0.5280	303.2
	0.9514	2.17	3.01	293.83	24.93	1.32	7.55	28.90	3.12	0.4996	286.9
	0.9508	2.12	3.00	299.29	19.47	1.36	7.77	28.48	3.54	0.4958	284.8
	0.9473			304.04	14.73	1.42	8.09	30.12	1.89	0.5322	305.7
	0.9478			298.35	20.41	1.40	7.97	30.13	1.88	0.5297	304.2
	0.9489			293.20	25.57	1.41	8.03	30.09	1.92	0.5251	301.6
	0.9556	1.98	2.89	298.97	19.80	1.25	7.15	27.56	4.45	0.4682	268.9
3monomer	0.9537	2.09	2.89	294.10	24.67	1.29	7.34	28.40	3.61	0.4841	278.0
	0.9544	2.14	2.92	293.30	25.47	1.29	7.35	28.37	3.64	0.4801	275.7
	0.9469			301.15	17.62	1.43	8.13	30.24	1.77	0.5342	306.8
	0.9470			302.38	16.39	1.43	8.12	30.25	1.76	0.5340	306.7
	0.9490	2.34	3.12	300.88	17.89	1.38	7.89	29.55	2.46	0.5141	295.3
	0.9541	2.11	2.95	284.74	34.02	1.29	7.34	28.43	3.59	0.4832	277.5
	0.9464			305.33	13.44	1.44	8.19	30.38	1.63	0.5370	308.4
	0.9542			292.00	26.77	1.30	7.40	28.47	3.54	0.4809	276.2
	0.9468			304.03	14.74	1.43	8.16	30.14	1.87	0.5342	306.8
	0.9480			299.05	19.71	1.40	7.99	30.11	1.90	0.5282	303.3
	0.9577	1.94	2.82	290.87	27.89	1.23	7.00	27.27	4.74	0.4531	260.2
	0.9550	2.04	2.89	293.77	24.99	1.29	7.34	27.98	4.03	0.4738	272.1

Note: R(O-H), R(H···O) and R(O···O) are the O-H bond length, the H···O distance and the O···O distance, respectively, for the Si-O-H···O linkage; only hydrogen bonds with R(H···O)≤2.6 Å (R(O···O)≤3.3 Å) are tabulated

[a] Numbers denote the Si-O-Si angle

[b] δ_i^O relative to H_2O; the $\Delta\sigma^O$ for SiOH in all the calculated silicate clusters are in the range 34–60 ppm; their ^{17}O *EFG* asymmetry η are in the range 0.45–0.60. All the calculated silicate clusters have negative ^{17}O *QCC* values; all ^{17}O *QCC* values normalized to the experimental value of H_2O

[c] δ_i^H relative to TMS; the $\Delta\sigma^H$ for SiOH in all the calculated silicate clusters are between 20–28 ppm; their ^{2}H *EFG* asymmetry η have a small range of 0.05–0.08; all ^{2}H *QCC* values normalized to the experimental value of $^{2}H_2O$

[d] The first three lines are for hydroxyls (OH) linked to the end Si (Q^1) and the fourth linked to the central Si(Q^2)

bonding is only moderate. In order to evaluate better how hydrogen bonding affect the ^{17}O and ^{1}H (^{2}H) NMR properties of silanols, we have also studied the simplified cases of two- and three- $Si(OH)_4$ monomers in free contact, with geometries optimized to give an energy minimum. The actual hydrogen bonding situation in silicates is probably complex and may vary between these two extreme cases (see Sauer et al. 1994). For the two- interacting $Si(OH)_4$ monomer geometry, there are three hydrogen bonds between the two monomers with O···H distances of 1.98, 2.12 and 2.17 Å (Fig. 1). The distances for all the other O···H pairs are ≥2.66 Å. The O-H bond lengths range from 0.947 Å to 0.956 Å. For the three- interacting $Si(OH)_4$ monomer geometry, there are six hydrogen bonds among the three monomers with O···H distances ranging from 1.94 to 2.34 Å: four of the hydroxyls each form two hydrogen bonds both as a hydrogen donor (O-H···O) and as a hydrogen acceptor (H···O-H), and four others each form a single hydrogen bond (Fig. 1). The O-H bond lengths range from 0.946 Å to 0.958 Å.

For all the studied clusters, the O-H bond length of the silanols in general increases with increasingly strong hydrogen bonding to a second O (Si-O-H···O). The latter can be described by either the H···O distance or the O···O distance, which are linearly correlated with each other.

^{29}Si chemical shift

For tetrahedral silicates, it is known from experimental NMR studies that the ^{29}Si chemical shift largely depends on the tetrahedral connectivity, two aspects of which are the degree of polymerizations and the intertetrahedral angle. The former is often described by the Q^n terminology (where n=0–4): a Si of Q^n speciation has n tetrahedral cations (e.g., Si, Al) as the next-nearest neighbors. The Si at-

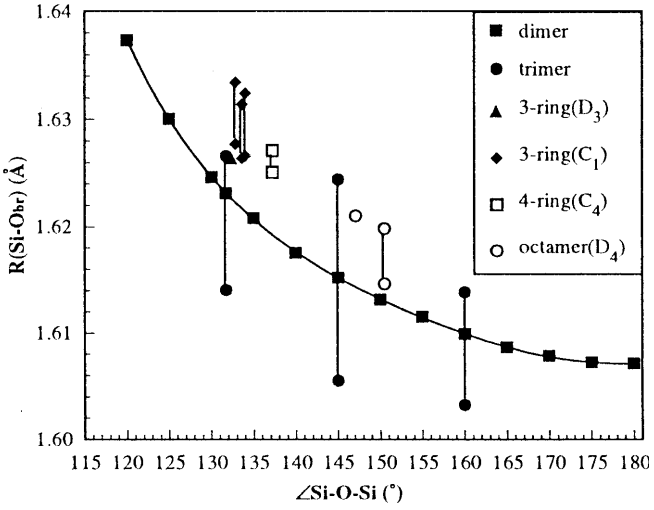

Fig. 2 Si-O_{br} bond length, R(Si-O_{br}), as a function of Si-O-Si angle for $Si_2O(OH)_6$ dimer, $Si_3O_2(OH)_8$ linear trimer, $Si_3O_3(OH)_6$ three-membered rings (D_3 and C_1 symmetries), $Si_4O_4(OH)_8$ four-membered ring and $Si_8O_{12}(OH)_8$ octamer. Individual Si-O_{br} bond lengths, instead of the average values, are plotted. *Vertical lines* connect data for each Si-O-Si linkage

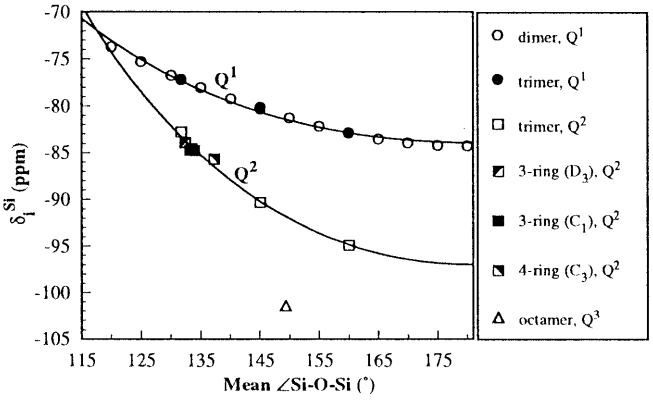

Fig. 3 ^{29}Si isotropic chemical shift (δ_i^{si}) as a function of the mean Si-O-Si angle (α) for $Si_2O(OH)_6$ dimer, $Si_3O_2(OH)_8$ linear trimer, $Si_3O_3(OH)_6$ three-membered rings (D_3 and C_1 symmetries), $Si_4O_4(OH)_8$ four-membered ring and $Si_8O_{12}(OH)_8$ octamer. Regression of all the data for Q^1 yields: δ_i^{si} (Q^1)=–65.0lcosα/(cosα–1)–51.40 (ppm), with a square of regression coefficient R^2=0.991; regression of all the data for Q^2 yields: δ_i^{si} (Q^2)=–136.lcosα/(cosα–1)–28.95 (ppm), with R^2=0.988

oms in the $Si(OH)_4$ monomers corresponds to Q^0 in the Q^n terminology. All the Si atoms in the $Si_2O(OH)_6$ dimers and the two end Si in the $Si_3O_2(OH)_8$ linear trimers correspond to Q^1. All the Si in the three- and four- membered rings and the central Si in the $Si_3O_2(OH)_8$ linear trimers correspond to Q^2. The Si atoms in the $Si_8O_{12}(OH)_8$ octamer correspond to Q^3. The calculated ^{29}Si isotropic chemical shifts, δ_i^{Si} are in the range –70.4∼–72.9 ppm for Q^0, –73.7∼–84.3 ppm for Q^1, –82.8∼–95.0 ppm for Q^2 and –101.4 ppm for Q^3 (Table 3). These are within the respective range of Si in Q^0 (–60∼–90 ppm), Q^1 (–68.4 ∼–96.9 ppm), Q^2 (–73.8∼–97.6 ppm) and Q^3 (–73 ∼–110 ppm) sites of silicate minerals (see compilations in Stebbins 1995). These results are also in good agreement with those of Moravetski et al. (1996) calculated with the TZP basis set and with the result for Q^2 in a $Si_3O_2(OH)_8$ linear trimer with Si-O-Si angles of 144° calculated by Sykes et al. (1997) with the 6–311+G(d,p) basis set, both basis sets are similar to the one used in the present study.

The δ_i^{Si} of both Q^1 and Q^2 become more negative with increasing Si-O-Si angle (Fig. 3), consistent with experimental data for Q^4 in tectosilicates. Correlations between δ_i^{Si} and Si-O-Si angle are in general poor for Q^1 and Q^2 sites in silicate minerals, because δ_i^{Si} is also affected by other structural parameters and in particular by the type of network-modifying cations (e.g., Na, K, Ca, Mg). Our calculations for small clusters are probably better compared with data for tectosilicates that lack such network-modifying cations. Linear correlations between δ_i^{Si} and several functions of Si-O-Si angle (α) such as the mean α, cosα/(cosα–1) and secα, have been suggested based on data on silica polymorphs and zeolites (mostly within the angle range 140°–160°) (e.g., Smith and Blackwell 1983; Engelhardt and Redeglia 1984; Ramdas and Klinowski 1984; Oestrike et al. 1987). Our calculations for Q^1 in the dimers and linear trimers show that whereas nearly linear correlation between δ_i^{Si} and all these functions are valid when only data in the range of 140°–160° are considered, there is a significant deviation from linearity between δ_i^{Si} and α when all data from 120° to 180° are included (see Fig. 3). The slope $d\delta_i^{Si}/d\alpha$ within the 140°–160° range is –0.183 ppm/deg for Q^1, about 1/3.3 of the slope for Q^4 derived from experimental data on silica and zeolites (e.g., –0.619 in Engelhardt and Radeglia 1984; and –0.589 in Oestrike et al. 1987). If bond additivity is obeyed, one might expect the $d\delta_i^{Si}/d\alpha$ slope for Q^1 to be 1/4 of the slope for Q^4. The slight deviation from 1/4 may be largely attributed to scattering of the experimental data caused by other structural variations and/or errors of the experimental data. The calculated $d\delta_i^{Si}/d\alpha$ slope for Q^2 is roughly twice of that for Q^1 (see Fig. 3), conforming with bond additivity. When all data for Q^1 in the dimers and linear trimers from 120° to 180° are considered, we found that linear regression of δ_i^{Si} with the function cosα gives the best fit, leading to the following equation: δ_i^{Si} (Q^1)=21.03cosα–63.19 (ppm), with a square of regression coefficient R^2 =0.9993. Linear regression with the function cosα/(cosα–1) gives a somewhat larger R^2 of 0.991 with the following equation: δ_i^{Si} (Q^1)=–65.01cosα/(cosα–1) –51.40 (ppm) (shown in Fig. 3). For Q^2, the calculated δ_i^{Si} show obvious scattering in the δ_i^{Si} versus α plot among clusters of different symmetries. A linear regression with either functions give similar R^2. The function for cosα/(cosα–1) is as follows: δ_i^{Si} (Q^2)=–136.1cosα/(cosα–1) –28.95 (ppm), with R^2=0.988. The functional dependence of δ_i^{Si} on α probably vary with the choice of basis sets.

The ^{29}Si shielding anisotropy ($\Delta\sigma^{Si}=\sigma_{33}-(\sigma_{11}+\sigma_{22})/2$; where σ_{11}, σ_{22} and σ_{33} are the ^{29}Si shielding tensor components with $|\sigma_{33}|\geq|\sigma_{11}|\geq|\sigma_{22}|$) for all the Si in the Q^1 sites

range from 17.2 ppm to 22.5 ppm (see Table 3). It increases from 120° to 125° (Si-O-Si angle) and then decreases monotonously to 180° for the $Si_2O(OH)_6$ dimers. The principle axes of the chemical shift tensor do not coincide with the molecular symmetry axes. The largest component is at a small angle to the molecular axis lying in the SiOSi plane and perpendicular to the C_2 axis for the dimers. The ^{29}Si shielding anisotropy for Si in the Q^2 sites are in a wider range from –25.0 to 37.3 ppm, and that of the Si in the Q^3 sites of the $Si_8O_{12}(OH)_8$ octamer gives the largest value of 39.9 ppm (see Table 3).

^{17}O chemical shift and electric field gradient (EFG) parameters

Bridging oxygens (BO) in the Si-O-Si linkages

The calculated ^{17}O isotropic chemical shift (δ_i^O) (relative to H_2O molecule) for all the bridging oxygens in the $Si_2O(OH)_6$ dimers, $Si_3O_2(OH)_8$ linear trimers, $Si_3O_3(OH)_6$ three-membered rings, $Si_4O_4(OH)_8$ four-membered rings and $Si_8O_{12}(OH)_8$ octamer are in the range from 35.6 to 52.8 ppm. All the reported experimental δ_i^O data (relative to liquid H_2O) for bridging oxygens in the Si-O-Si linkages in silicate minerals and solutions range from 40 to 87 ppm (see Stebbins 1995 for compilations of data for minerals, also see Fig. 5). The agreement between the calculations and experiments is reasonably good considering the possible variations in the gas-condensed phase δ_i^O shifts between silicates and H_2O, the chemical shift reference.

In all the calculated silicate clusters, the $O_{br}\cdots H$ distances are ≥2.66 Å, thus hydrogen bonding are probably negligible for these bridging oxygens and each bridging oxygen may be considered to be bonded only to two cations (Si), similar to those in silica. In contrast, bridging oxygens in depolymerized silicates (minerals, glasses, or solutions) are in general also bonded to one or more network-modifying cations. Thus, although from the standpoint of tetrahedral polymerization, these clusters appear to resemble depolymerized silicates, the local oxygen coordinations are actually similar to those of tectosilicates. The available experimental δ_i^O data for silica and zeolites are in a small range from 40 to 52 ppm (see compilations in Stebbins 1995), in good agreement with our calculations.

For the $Si_2O(OH)_6$ dimers, the calculated δ_i^O of the bridging oxygens decreases monotonously with increasing Si-O-Si angle by 14.5 ppm from 120° to 180° (see Table 4, Fig. 4). There is a linear correlation between the δ_i^O and the parameter, cosα/(cosα–1), for the degree of s hybridization of the oxygen bond orbitals (Fig. 4), giving the following equation: δ_i^O=–87.9cosα/(cosα–1)+79.4, with R^2=0.9999. The slope is slightly larger than that of the δ_i^{Si} versus cosα/(cosα–1) correlation for Q^1 (–65.0), but smaller than the same slope for Q^2 (–136.1), and even smaller than that of Q^4 (–247.05: Engelhardt and Radeglia 1984). For example, a 5° increase in mean Si-O-Si angle from 145° to 150° corresponds to a 3-ppm decrease in δ_i^{Si} for Q^4, but to only about 1.3-ppm decrease in δ_i^O. Thus, ^{17}O chemical shift is a less sensitive probe of the Si-O-Si angle than ^{29}Si chemical shift for tectosilicates.

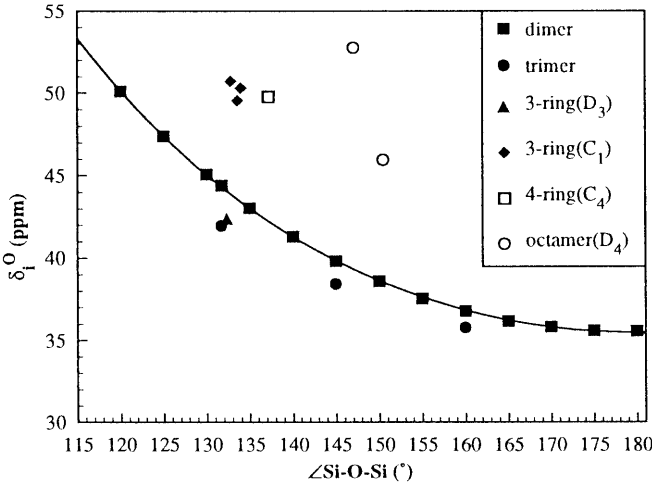

Fig. 4 ^{17}O isotropic chemical shift (δ_i^O) as a function of Si-O-Si angle (α) for bridging oxygens (Si-O-Si) in $Si_2O(OH)_6$ dimer, $Si_3O_2(OH)_8$ linear trimer, $Si_3O_3(OH)_6$ three-membered rings (D_3 and C_1 symmetries), $Si_4O_4(OH)_8$ four-membered ring and $Si_8O_{12}(OH)_8$ octamer. Regression of the data for the dimers yields: δ_i^O=–87.9cosα/(cosα–1)+79.4, with R^2=0.9999

The δ_i^O for all the other silicate clusters do not fall on the same trend as the $Si_2O(OH)_6$ dimer in the δ_i^O versus α plot (see Fig. 4), indicating that other structural parameters also affect δ_i^O. It is generally known that chemical shift is dominated by nearest neighbor (NN) and next-nearest neighbor (NNN) effects. In the case of ^{29}Si chemical shift, the next-nearest neighbor effect leads to different (though overlapping) chemical shift ranges for Si of different Q^n speciations (see discussions earlier). For a bridging oxygen in the Si(Q^n)-O-Si($Q^{n'}$) linkage in tetrahedral silicates, there are six NNN oxygens, among which the number of BOs can be easily shown to be n+n'–2, varying from 0 for Si(Q^1)-O-Si(Q^1) to 6 for Si(Q^4)-O-Si(Q^4). One might thus expect that the δ_i^O of bridging oxygens varies systematically with the number of the NNN bridging oxygens (NNN-BO), or equivalently, the Q^n speciations of the nearest neighbor Si. The number of NNN-BO for the bridging oxygens increases from 0 in the dimers, to 1 in the linear trimers, to 2 in the rings, and then to 3 in the octamer (double rings). However, our calculations show that the bridging oxygens in the various linkages do not give distinct δ_i^O ranges. For example, data for the linear trimers and rings fall on either side of the correlation for the dimers in the the δ_i^O versus α plot (see Fig. 4). One factor that causes such overlapping seems to be the cluster symmetry. For example, the δ_i^O values for the bridging oxygens in the two types of three-membered rings that have similar Si-O-Si angles, but different symmetries differ by as much as 8.3 ppm (over one half of the total Si-O-Si angle dependence for the dimers from 120° to 180°) (see Fig. 4). Apparently, bridging oxygens

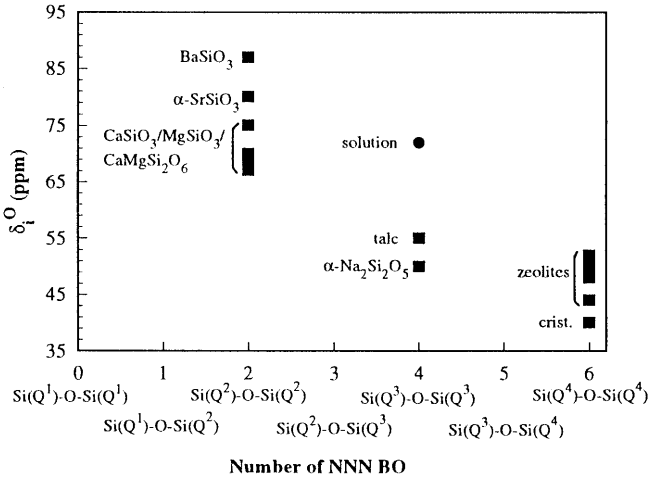

Fig. 5 ^{17}O isotropic chemical shift (δ_i^O) as a function of the number of next-nearest neighbor (NNN) BO for bridging oxygens in the Si-O-Si linkages in zeolites (Timken et al. 1986a, b), SiO_2 cristobalite (Spearing et al. 1992), $Mg_3Si_4O_{10}(OH)_2$ talc (Walter et al. 1988); α-$Na_2Si_2O_5$ (Xue et al. 1994); $CaMgSi_2O_6$ diopside, $MgSiO_3$ clinoenstatite, $Ca_3Si_3O_9$ wollastonite (Mueller et al. 1992), α-$CaSiO_3$ pseudo-wollastonite, α-$SrSiO_3$ and $BaSiO_3$ (Timken et al. 1987), as well as in cubic octameric cage $[Si_8O_{20}]^{8-}$ anion from concentrated methanolic tetramethylammonium silicate solution (Knight et al. 1989). There is a general trend of decreasing δ_i^O with increasing number of NNN BO

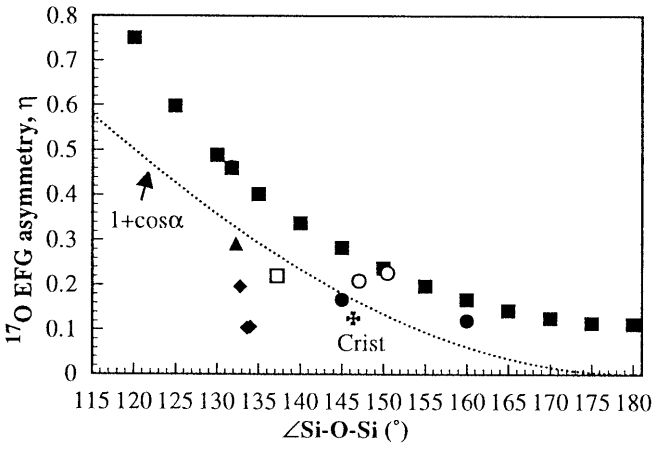

Fig. 6 ^{17}O *EFG* asymmetry parameter, η as a function of Si-O-Si angle for bridging oxygens (Si-O-Si) in $Si_2O(OH)_6$ dimer, $Si_3O_2(OH)_8$ linear trimer, $Si_3O_3(OH)_6$ three-membered rings (D_3 and C_1 symmetries), $Si_4O_4(OH)_8$ four-membered ring and $Si_8O_{12}(OH)_8$ octamer. Also shown is the curve, η=1+cosα, derived by Farnan et al. (1992) from ab initio results of Tossell and Lazzeretti (1988). Experimental data for cristobalite (Spearing et al. 1992) are also shown. *Symbols* for the clusters are identical to those in Fig. 4

in puckered ring structures (three-membered ring with C_1 symmetry, four-membered ring with C_4 symmetry and octamer with D_4 symmetry) yield larger δ_i^O than those in planner rings with similar Si-O-Si angles (see Fig. 4). Thus, the influence of symmetry on the δ_i^O is large and it would not be rewarding to try to infer the Si-O-Si angle distribution information from the δ_i^O data alone.

In contrast to ^{29}Si NMR, there have been few discussions of empirical correlations between ^{17}O NMR chemical shift of bridging oxygens (Si-O-Si) and local structure based on experimental data. In order to compare with our calculations, we have compiled the available experimental ^{17}O NMR data for crystalline silicates and silicate solution (Fig. 5). These data show a general trend of decreasing δ_i^O with increasing number of NNN BO (increasing polymerizations). The δ_i^O range for bridging oxygens with a given number of NNN BO seems to be large, despite of the scarcity of the data. For example, the δ_i^O of bridging oxygens in ring and chain silicates (number of NNN BO=2), for which the most experimental data are available, cover a range of 20 ppm. This is mostly a result of variations in the type of network-modifying cations for depolymerized silicates. The total δ_i^O range of all the experimental data for bridging oxygens are about 47 ppm, much larger than that of the small clusters from our calculations. As noted already, in depolymerized silicates, bridging oxygens are in general also coordinated to one or more network-modifying cations in addition to two Si. The δ_i^O variation with the degree of polymerization and with the type of network-modifying cations in silicate minerals and solutions probably reflect, to a large extent, the direct interaction between bridging oxygens and the network-modifying cations.

The ^{17}O EFG asymmetry parameter η has been suggested to be a good probe to the Si-O-Si angle distributions, from previous ab initio calculations on Si_2OH_6 dimers with C_{2v} symmetry (and D_{3h} symmetry in the straight Si-O-Si case) at the 3–21G(d) and 3–21G(d,p) levels (Tossell and Lazzeretti 1988; Tossell 1990). The relationship, η=1+cosα, derived from such calculations has been used to infer the Si-O-Si angle distribution in silicate glasses (Farnan et al. 1992). The calculated η values for bridging oxygens in the $Si_2O(OH)_6$ dimers with C_2 symmetry from our study also show a monotonous decrease with increasing Si-O-Si angle, but deviate from linearity with the functions cosα, secα or cosα/(cosα–1), although the curvature is small in the latter two cases. Moreover, the calculated η values for bridging oxygens in these dimers are consistently higher by about 0.1 than those of Tossell and Lazzeretti (1988) (see Fig. 6). This discrepancy is probably largely attributable to the difference in point symmetry of the dimers. For example, the ^{17}O EFG asymmetry parameter η is constrained to be 0 by symmetry in the case of D_{3h} symmetry for the straight Si-O-Si angle geometry; whereas the calculated *EFG* η value for $Si_2O(OH)_6$ dimer with C_2 symmetry and with the same Si-O-Si angle is 0.112. The calculated *EFG* η values for bridging oxygens in the other silicate clusters are also in general lower than the η versus α correlation for the $Si_2O(OH)_6$ dimer (see Fig. 6). In particular, the *EFG* η for bridging oxygens in the two types of $Si_3O_3(OH)_6$ three-membered rings with C_1 and D_3 symmetries do not show obvious correlation with Si-O-Si angle. This again suggests that the *EFG* η of the bridging oxygens is largely influenced by the local symmetry of

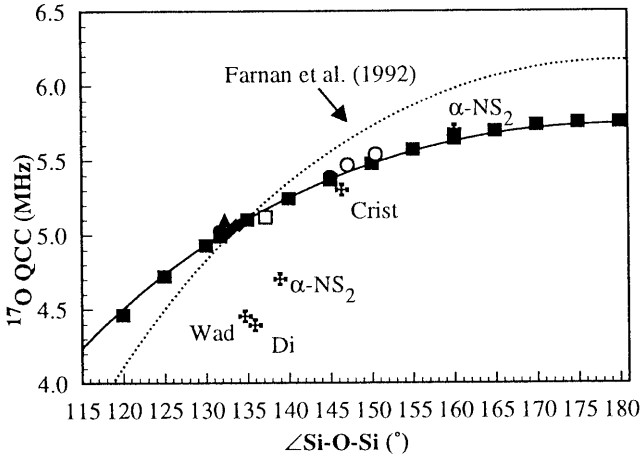

Fig. 7 ^{17}O *QCC* as a function of Si-O-Si angle (α) for bridging oxygens (Si-O-Si) in $Si_2O(OH)_6$ dimer, $Si_3O_2(OH)_8$ linear trimer, $Si_3O_3(OH)_6$ three-membered rings (D_3 and C_1 symmetries), $Si_4O_4(OH)_8$ four-membered ring and $Si_8O_{12}(OH)_8$ octamer. Regression of the data for the dimers yields: QCC=7.43cosα/(cosα–1)+2.03, with R^2=0.9997. Also shown is the *curve* $QCC(\alpha)$=2QCC(180°)cosα/(cosα–1) (with $QCC(180°)$=6.17 MHz) adopted in Farnan et al. (1992), the slope of which was from ab initio calculations of Tossell and Lazzeretti (1988). Experimental data for SiO_2 cristobalite (Crist) (Spearing et al. 1992), $CaMgSi_2O_6$ diopside (Di) (Mueller et al. 1993), $K_2Si_4O_9$ wadeite (Wad) and α-$Na_2Si_2O_5$ (α–NS_2) (Xue et al. 1994) are also shown. *Symbols* for the clusters are identical to those in Fig. 4

the O site. Caution should thus be taken in predicting the Si-O-Si angle distribution from the ^{17}O *EFG* asymmetry parameter η, because the local site symmetry of bridging oxygens in real silicates is expected to vary. The *EFG* η versus α correlation defined by bridging oxygens in the $Si_2O(OH)_6$ dimers with C_2 symmetry probably represents an upper limit to the *EFG* η values of bridging oxygens in Si-O-Si linkages in general. The experimental data for cristobalite (η=0.125: Spearing et al. 1992, α=146.4°) falls within the range of the calculated values (see Fig. 6).

The ^{17}O *QCC* of bridging oxygens in the $Si_2O(OH)_6$ dimers, like δ_i^O, shows a linear correlation with the parameter for the degree of s hybridization of the oxygen bond orbital, cosα/(cosα–1) (see Fig. 7). Regression of the data yields the following equation: ^{17}O *QCC* (MHz)=7.43cosα/(cosα–1)+2.03, with R^2=0.9997. The slope is much smaller (about 60%) than that of Tossell and Lazzeretti (1988) calculated at the 3–21G(d) and 3–21G(d,p) levels for Si_2OH_6 dimers with a fixed Si-O bond length. The latter has been adopted in Farnan et al. (1992) ($QCC(\alpha)$=2QCC(180°)cosα/(cosα–1), with $QCC(180°)$ =6.17 MHz)) to interpret the Si-O-Si angle distribution in a $K_2Si_4O_9$ glass (see Fig. 7). Our calculations have been performed with much larger basis sets on optimized geometries, and thus should be more reliable. In Fig. 7, it is shown that our calculated ^{17}O *QCC* values for bridging oxygens agree very well with the experimental ^{17}O *QCC* data for SiO_2 cristobalite (5.3 MHz: Spearing et al. 1992). Agreement with more recent experimental ^{17}O NMR data for SiO_2 coesite (Grandinetti et al. 1995) is also excellent.

Unlike the ^{17}O chemical shift or the ^{17}O *EFG* asymmetry parameter η, the ^{17}O *QCC* for bridging oxygens in the other calculated clusters from the linear trimers to octamer all fall on the trend defined by the $Si_2O(OH)_6$ dimers (see Fig. 7). Neither the Q^n speciations of the two Si atoms to which the bridging oxygens are linked, nor the local symmetry exhibit any significant effect on the ^{17}O *QCC*. Furthermore, the fact that the average Si-O_{br} bond lengths for most of these silicate clusters differ from those of the dimers (see Fig. 2) implies that the Si-O_{br} bond length dependence of ^{17}O *QCC* is probably also weak. These results thus suggest that ^{17}O *QCC* of bridging oxygens (Si-O-Si) is the most reliable ^{17}O NMR parameter that may be used to predict Si-O-Si angle distribution in silicates with varying local symmetries or Si-O_{br} bond lengths.

It should be emphasized again that these results are for bridging oxygens that are coordinated only to two cations (Si), and therefore are directly applicable only to tectosilicates. Experimental ^{17}O NMR studies have shown that the presence of network-modifying cations, such as Na and Ca, in depolymerized silicates, tend to lower the ^{17}O *QCC* of bridging oxygens, possibly because the interaction of such cations increase the ionicity of the Si-O bond (see Timken et al. 1986a, b, 1987). It is also clear from Fig. 7 that whereas the experimental ^{17}O *QCC* value for SiO_2 cristobalite is close to the correlation from this study, data for bridging oxygens (Si-O-Si) in silicates containing network-modifying cations, such as $CaMgSi_2O_6$ diopside, $K_2Si_4O_9$ wadeite and α-$Na_2Si_2O_5$, are in general lower (see Fig. 7). Reinterpretation of the two-dimensional DAS data for $K_2Si_4O_9$ glass by Farnan et al. (1992) based on such calculations is thus not attempted, but our calculations would be very useful if similar data for SiO_2 glasses are available.

Whereas the correlation of ^{17}O *QCC* for the bridging oxygens with Si-O-Si angle is useful in predicting Si-O-Si angle distribution in disordered silicates, as illustrated by the two-dimensional DAS study of Farnan et al. (1992), the small slope of this correlation also implies that it is not sensitive to small changes in the Si-O-Si angle. For example, Spearing et al. (1992) has observed a 3-ppm drop in δ_i^{Si} across the transition from α- to β- SiO_2 cristobalite, but failed to detect any change in ^{17}O *QCC* (QCC=5.3±0.1 MHz). From the discussion of ^{29}Si chemical shift, a 3-ppm drop in δ_i^{Si} corresponds roughly to a 5° increase in the mean Si-O-Si angle for SiO_2. Our calculation suggests that with a 5°-increase in Si-O-Si angle near 146°, ^{17}O *QCC* increases by only about 0.1 MHz, within the experimental uncertainty, consistent with the result of Spearing et al. (1992).

The principle axes of the ^{17}O *EFG* tensor for bridging oxygens in the $Si_2O(OH)_6$ dimers coincide with the molecular symmetry axes, with the largest component lying in the SiOSi plane perpendicular to the C_2 axis; whereas those of the other clusters do not coincide with the molecular symmetry axes.

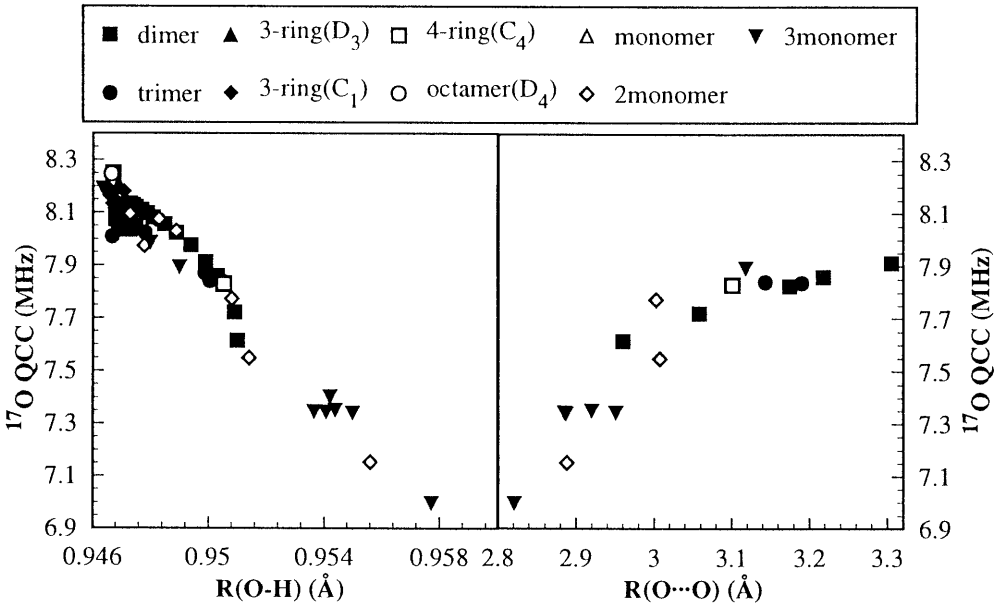

Fig. 8 ^{17}O *QCC* as a function of O-H bond length, *R*(O-H) (*left*) and the O···O distance of the hydrogen bond (Si-O-H···O), *R*(O···O) (*right*), for silanols (SiOH) in $Si_2O(OH)_6$ dimer, $Si_3O_2(OH)_8$ linear trimer, $Si_3O_3(OH)_6$ three-membered rings (D_3 and C_1 symmetries), $Si_4O_4(OH)_8$ four-membered ring, $Si_8O_{12}(OH)_8$ octamer, isolated $Si(OH)_4$ monomer and two- and three- interacting $Si(OH)_4$ monomers

Silanol oxygens in the Si-O-H linkages

The ^{17}O *QCC* for silanol oxygens in all the studied clusters (isolated) are in the range of 7.6–8.3 MHz (Table 4), much larger than those of bridging oxygens (Si-O-Si). The data exhibit no obvious correlation between ^{17}O *QCC* of the hydroxyls and the Q^n speciation of the Si in the Si-O-H linkages. For example, the ^{17}O *QCC* value for $Si(Q^0)$-O-H in the isolated $Si(OH)_4$ monomer (8.1 MHz) is similar to that for $Si(Q^3)$-O-H in the $Si_8O_{12}(OH)_8$ octamer (8.3 MHz). It has been shown from experimental NMR studies that nonbridging oxygens (Si-O-M, where M=Na, K, Ca, Mg,...) have much smaller ^{17}O *QCC* values (1.6–3.2 MHz) than bridging oxygens (3.7–5.8 MHz) (e.g., Timken et al. 1986a, b, 1987; Walter et al. 1988; Mueller et al. 1992; Xue et al. 1994). Thus, the ^{17}O *QCC* of the Si-O-H linkages are very different from those of nonbridging oxygens in the normal sense.

There have been few ^{17}O NMR experimental data reported for silanols, although such groups are often present in hydrous silicates and silicate solutions. Walter et al. (1988) have reported that the Al^{VI}-O-H site (where Al^{VI} stands for Al coordinated to six O) gives a much broader ^{17}O NMR peak (greater *QCC*) and smaller chemical shift than the Al^{VI}-O-Al^{VI} site in boehmite(AlO(OH)), a trend consistent with our calculations for silicates. In the same paper, these authors have also detected a ^{17}O NMR peak from cross-polarization studies of an amorphous silica sample, which they attributed to silanol oxygens. The simulated parameters for this peak were: ^{17}O *QCC*=4 MHz, ^{17}O *EFG* asymmetry parameter η=0.3 and δ_i^O=20 ppm. The ^{17}O *QCC* value of this peak is thus much smaller than our calculated values for silanols, but is similar to those of bridging oxygens.

It is known that hydroxyls may interact with each other through hydrogen bonding on the surface and in the interior of silicates. To assess whether hydrogen bonding can significantly reduce the ^{17}O *QCC* values of silanols, we have calculated the NMR properties for two- and three-freely interacting $Si(OH)_4$ clusters. Because the calculated ^{17}O *QCC* of silanols do not show obvious dependence on the Q^n speciation of the Si, interacting monomers may be considered to be reasonable models for the more polymerized systems, such as silica, in terms of ^{17}O NMR properties. Our calculations show that the ^{17}O *QCC* of the silanols are indeed decreased by increasingly strong hydrogen bonding to a second O atom (Si-O-H···O), as described by the H···O distance or O···O distance (Fig. 8). However, even the lowest calculated ^{17}O *QCC* of the silanols (7.0 MHz) is still much larger than the value (4 MHz) suggested for silanols in amorphous silica by Walter et al. (1988), casting doubt on the interpretation of the latter data. Experimental ^{17}O NMR data on crystalline phases, such as $H_2Si_2O_5$, may help solve this issue.

It is also noted from Fig. 8 that the ^{17}O *QCC* values of silanols do not vary appreciably when the O···O distance approach 3.3 Å (corresponding to about 2.6-Å H···O distance), suggesting that such weak hydrogen bonding do not have significant effect on the ^{17}O *QCC* of silanols. This is also true for the ^1H chemical shift and ^2H *QCC* parameters of silanols described later (see Fig. 9). When data for all the silanols including those that lack effective hydrogen bonding are considered, there is a general trend of decreasing ^{17}O *QCC* with increasing O-H bond length (Fig. 8).

The calculated δ_i^O for silanols in all the silicate clusters are in the range 14.3∼34.0 ppm (Table 4), about 20–40 ppm lower than those of the bridging oxygens (35.6∼52.8 ppm). There is no obvious correlation between δ_i^O of the silanols and the Q^n speciation of the Si. Neither are there any simple correlations between δ_i^O and other structure parameters, such as the Si-O-H angle, the Si-OH bond length, the number or length of the hydrogen bonds.

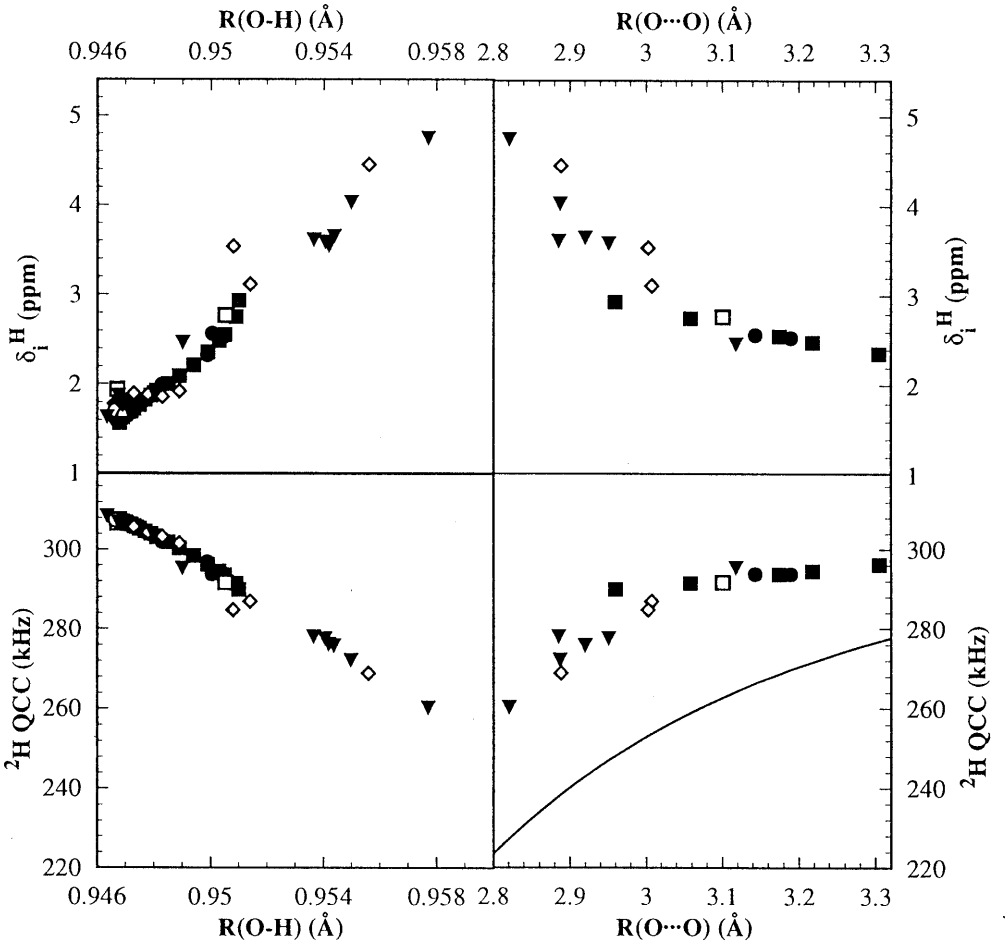

Fig. 9 ^{1}H isotropic chemical shift (δ_i^H: *top*) and ^{2}H QCC (*bottom*) as a function of O-H bond length, *R*(O-H) (*left*) and the O···O distance of the hydrogen bond (Si-O-H···O), *R*(O···O) (*right*), for silanols (SiOH) in $Si_2O(OH)_6$ dimer, $Si_3O_2(OH)_8$ linear trimer, $Si_3O_3(OH)_6$ three-membered rings (D_3 and C_1 symmetries), $Si_4O_4(OH)_8$ four-membered ring, $Si_8O_{12}(OH)_8$ octamer, isolated $Si(OH)_4$ monomer and two- and three-interacting $Si(OH)_4$ monomers. *Symbols* for the clusters are identical to those in Fig. 8. The *curve* in the *lower-right* figure is for the relation: ^{2}H *QCC*(kHz)=311.0–223.8/(*R*(O···O)–l.433)^3 derived from experimental data for non-silicates (see Eckert et al. 1987)

^{1}H chemical shift and ^{2}H *EFG* parameters of silanols

The ^{1}H isotropic chemical shifts (δ_i^H) for silanols in all the calculated silicate clusters (isolated) are in the range 1.56–2.93 ppm (see Table 4), consistent with the experimental δ_i^H range of 1.8–2.3 ppm for terminal SiOH in zeolites (see data in Pfeifer 1994). Our calculated δ_i^H value for the isolated $Si(OH)_4$ monomer (1.71 ppm) is close to, though somewhat lower than, the value (2.22 ppm) reported by Fleischer et al. (1993) calculated with the IGLO method using the [7 s,6p,2d/5 s,4p,1d/3 s,1p] basis set. Like δ_i^O, there is no obvious correlation between δ_i^H of the silanols and Q^n speciation of Si (see Fig. 9).

In experimental NMR studies of silica gels and zeolites, interacting (hydrogen-bonded) hydroxyls have been shown to give larger ^{1}H chemical shifts than those of isolated ones (see Pfeifer 1994). For example, ^{1}H CRAMPS study of silica gel (Bronnimann et al. 1988) gives three peaks centered at 1.7 ppm, 3.0 ppm (broad) and 3.5 ppm, which have been assigned to isolated silanols, hydrogen-bonded silanols and physisorbed water, respectively. Our calculations on two- and three- interacting $Si(OH)_4$ monomers indeed show that silanols that are hydrogen bonded to a second O (Si-O-H···O) give larger ^{1}H chemical shift (4.74 ppm for the silanol with the shortest hydrogen bond studied). In Fig. 9, we have plotted the δ_i^H as a function of the O···O distance of the hydrogen bond to a second O (Si-O-H···O), as well as the O-H bond length, *R*(O-H). The plot shows that δ_i^H increases with increasing O-H bond length and decreasing O···O distance. Similar correlations have been reported for experimental NMR data of organic and inorganic compounds other than silicates (e.g., Berglund and Vaughan 1980). Eckert et al. (1988) have fitted such experimental data with a linear equation:δ_i^H (ppm)=79.05–25.5R(O···O) (Å) (where *R*(O···O) stands for the O···O distance), and have used this correlation to estimate the O···O distances for hydroxyls in hydrous silicate glasses. However, these data are for protons in non-silicates with O···O distances mostly shorter than those of the silicate clusters studied here (and perhaps also mostly shorter than those of silicate glasses). Although our calculated δ_i^H values roughly agree with this equation for *R*(O···O) around 2.9–3.0 Å, the calculated δ_i^H data give a much smaller slope (around 7) for *R*(O···O) between 2.8 and 3.1 Å, and level off at even larger *R*(O···O). It is conceivable that there may be some discrepancies between the calculated *R*(O···O) for silanols in the silicate clusters and those in silicate minerals and glasses due to calculation limitations and possible gas-condensed phase differences. Nevertheless, it seems reasonable that the contribution to δ_i^H from hydrogen bonds becomes increasingly small at large *R*(O···O).

The ^{2}H *QCC* for silanols in all the clusters are in a small (48-kHz) range from 260 kHz to 308 kHz, and the ^{2}H *EFG* asymmetry parameter, η, is in a small range of 0.05∼0.08 (Table 4). Like ^{17}O *QCC* and δ_i^H, there is no obvious correlation between ^{2}H *QCC* of silanols and Q^n speciation of Si (see Fig. 9). The smaller ^{2}H *QCC* values are from silanols that are hydrogen-bonded to a second O atom. The ^{2}H *QCC* of silanols decreases with increasing O-H bond length and decreasing O···O distance, mirroring the changes in δ_i^H (see Fig. 9). Similar correlations between ^{2}H *QCC* and O···O distance have also been reported for experimental ^{2}H NMR data of organic and inorganic compounds other than silicates (see Eckert et al. 1987). The calculated R(O···O) dependence of the ^{2}H *QCC* (the d(*QCC*)/dR slope) for silanols in the silicate clusters agrees well with that of the experimental data for non-silicates, although the absolute ^{2}H *QCC* values from our calculations are higher by about 10% (20–30 kHz) (see Fig. 9). The agreement is reasonable considering that these simple cluster calculations have not taken into account the medium effect that contribute to the gas-condensed phase difference, or the thermal vibrations/rotations and isotope (^{1}H/^{2}H) substitutions that may affect the observed (average) O···O distances.

In brief, both the δ_i^H and the ^{2}H *QCC* of silanols show correlations with the O-H bond length as well as with the hydrogen bond length (as described by the H···O distance or the O···O distance of the Si-O-H···O linkage), but do not exhibit appreciable dependence on the Q^n speciation of Si.

Conclusions

We have shown that reliable ^{29}Si, ^{17}O and ^{1}H chemical shift and ^{17}O *QCC* values can be obtained for silicate clusters from ab initio calculations with the robust 6–311+G(2df,p) basis set.

Our calculated δ_i^{Si} for Si in Q^0, Q^1, Q^2 and Q^3 sites in these clusters are within the respective range for Si in similar local environments in silicate minerals. The calculated $d\delta_i^{Si}/d\alpha$ slope for Q^1 within the range 140–160° is slightly larger than 1/4 of that for Q^4 within a similar angle range from experimental data. The calculated $d\delta_i^{Si}/d\alpha$ slope for Q^2 is about twice of the value for Q^1, conforming with bond additivity.

The δ_i^O, the ^{17}O *EFG* asymmetry parameter η and the ^{17}O *QCC* of bridging oxygens (Si-O-Si) all exhibit good correlation with the Si-O-Si angle in the case of $Si_2O(OH)_6$ dimer. However, the former two parameters also depend strongly on other structural parameters, and on the symmetry, in particular. The δ_i^O and ^{17}O *EFG* asymmetry parameter η should thus be used with caution for Si-O-Si angle evaluations. On the other hand, the ^{17}O *QCC* of the bridging oxygens does not show significant variation with structural parameters other than the Si-O-Si angle, and is thus expected be the most reliable ^{17}O NMR parameter for predicting Si-O-Si angle distributions in silicates.

The calculated ^{17}O *QCC* of silanols (Si-O-H) are much larger than those of bridging oxygens (Si-O-Si) or non-bridging oxygens (Si-O-M: where M=Na, Mg...). Hydrogen-bonding to a second O atom (Si-O-H···O) tends to lower the ^{17}O *QCC* of the silanol oxygens, but not to a value as low as those of the bridging oxygens.

The calculated δ_i^H of silanols are consistent with experimental data for zeolites, silica gels and hydrous silicate glasses. Hydrogen-bonding to a second O (Si-O-H···O) is shown to increase the δ_i^H and lower the ^{2}H *QCC* of the silanols, consistent with experimental observations for non-silicates.

Acknowledgements We are grateful to D.G. Fraser and two anonymous reviewers for helpful comments. We also thank J.F. Stebbins for enlightening communications. The cluster structures are plotted using the PPC_MacMolplt software by Brett Bode. This study is supported by the Grant-in-Aid for Scientific Research 08454153, the Ministry of Education, Science, Sports and Culture of Japan to MK.

References

Berglund B, Vaughan RW (1980) Correlations between proton chemical shift tensors, deuterium quadrupole couplings, and bond distances for hydrogen bonds in solids. J Chem Phys 73: 2037–2043

Bronnimann C, Zeigler RC, Maciel GE (1988) Proton NMR study of dehydration of the silica gel surface. J Am Chem Soc 110:2023–2026

Cheeseman JR, Trucks GW, Keith TA, Frisch MJ (1996) A comparison of models for calculating nuclear magnetic resonance shielding tensors. J Chem Phys 104:5497–5509

Chmelka BF, Zwanziger JW (1994) Solid-state NMR line narrowing methods for quadrupolar nuclei: double rotation and dynamic-angle spinning. In: Diehl P, Fluck E, Günther H, Kosfeld R, Seeing J (ed) NMR basic principles and progress, vol 33, Springer-Verlag, Berlin Heidelberg New York, pp79–124

Cong X, Kirkpatrick RJ (1993) ^{17}O and ^{29}Si MAS NMR study of β-C_2S hydration and the structure of calcium-silicate hydrates. Cem Concr Res 23:1065–1077

Eckert H, Yesinowski JP, Stolper EM, Stanton TR, Holloway J (1987) The state of water in rhyolitic glasses, a deuterium NMR study. J Non-Cryst Solids 93:93–114

Eckert H, Yesinowski JP, Silver LA, Stolper EM (1988) Water in silicate glasses: quantitation and structural studies by ^{1}H solid echo and MAS-NMR methods. J Phys Chem 92:2055–2064

Engelhardt G, Koller H (1994) ^{29}Si NMR of inorganic solids. In: Diehl P, Fluck E, Günther H, Kosfeld R, Seeing J (ed) NMR basic principles and progress, vol 33, Springer-Verlag, Berlin Heidelberg New York, pp1–30

Engelhardt G, Radeglia R (1984) A semi-empirical quantum-chemical rationalization of the correlation between SiOSi angles and ^{29}Si NMR chemical shifts of silica polymorphs. Chem Phys Lett 108:271–274

Farnan I, Grandinetti PJ, Baltisberger JH, Stebbins JF, Werner U, Eastman MA, Pines A (1992) Quantification of the disorder in network-modified silicate glasses. Nature 358:31–35

Fleischer U, Kutzelnigg W, Bleiber A, Sauer J (1993) ^{1}H NMR chemical shift and intrinsic acidity of hydroxyl groups. Ab initio calculations on catalytically active sites and gas-phase molecules. J Am Chem Soc 115:7833–7838

Florin AE, Alei M Jr (1967) ^{17}O NMR shifts in $H_2{}^{17}O$ liquid and vapor. J Chem Phys 47:4268–4269

Frisch MJ, Trucks GW, Schlegel HB, Gill PMW, Johnson BG, Robb MA, Cheeseman JR, Keith TA, Petersson GA, Montgomery JA, Raghavachari K, Al-Laham MA, Zakrzewski VG, Ortiz JV,

Foresman JB, Cioslowski J., Stefanov BB, Nanayakkara, A, Challacombe M, Peng CY, Ayala PY, Chen W, Wong, MW, Andres JL, Replogle ES, Gomperts R, Martin RL, Fox DJ, Binkley JS, Defrees DJ, Baker J, Stewart JP, Head-Gordon M, Gonzalez C, Pople JA (1995) Gaussian 94 (Revision B.2), Gaussian, Pittsburgh, PA, USA

Grandinetti PJ, Baltisberger JH, Farnan I, Stebbins JF, Werner U, Pines A (1995) Solid-state ^{17}O magic-angle and dynamic-angle spinning NMR study of the SiO_2 polymorph coesite. J Phys Chem 99:12341–12348

Janes N, Oldfield E (1985) Prediction of silicon-29 nuclear magnetic resonance chemical shifts using a group electronegativity approach: applications to silicate and aluminosilicate structures. J Am Chem Soc 107:6769–6775

Kanzaki M (1996) Ab initio calculation of ^{29}Si NMR chemical shifts for the clusters of $Si(OH)_4$, $Si(OH)_5^-$ and $Si(OH)_6^{-2}$. Mineral J 18:1–8

Keith, TA, Bader, RFW (1993) Calculation of magnetic response properties using a continuous set of gauge transformations. Chem Phys Lett 210, 223–231

Kelly HP (1969) Hyperfine structure of oxygen calculated by many-body theory. II. Phys Rev 180:55–61

Kintzinger J-P, 1981. Oxygen NMR characteristic parameters and applications. In: Diehl P, Fluck E, Kosfeld R (ed) NMR basic principles and progress, vol 17, Springer-Verlag, Berlin Heidelberg New York, pp1–64

Knight CTG, Thompson AR, Kunwar AC, Gutowsky HS, Oldfield E (1989) Oxygen-17 nuclear magnetic resonance spectroscopic studies of aqueous alkaline silicate solutions. J Chem Soc Dalton Trans 1989:275–281

Kubicki JD, Sykes D (1993) Molecular orbital calculations of vibrations in three-membered aluminosilicate rings. Phys Chem Minerals 19:381–391

Malkin VG, Malkina OL, Steinebrunner G, Huber H (1996) Solvent effect on the NMR chemical shieldings in water calculated by a combination of molecular dynamics and density functional theory. Chem Eur J 2:452–457

Moravetski V, Hill J-R, Eichler U, Cheetham AK, Sauer J (1996) ^{29}Si NMR chemical shifts of silicate species: Ab initio study of environment and structural effects. J Am Chem Soc 118, 13015–13020

Mueller KT, Baltisberger JH, Wooten EW, Pines A (1992) Isotropic chemical shifts and quadrupolar parameters for oxygen-17 using dynamic-angle spinning NMR. J Phys Chem 96:7001–7004

Oestrike R, Yang W-H, Kirkpatrick RJ, Hervig RL, Navrotsky A, Montez B (1987) High-resolution ^{23}Na, ^{27}Al, and ^{29}Si NMR spectroscopy of framework aluminosilicate glasses. Geochim Cosmochim Acta 51:2199–2209

Olah GA, Li X-Y, Wang Q, Rasul G, Surya Prakash GK (1995) Trisilyloxonium ions: Preparation, NMR spectroscopy, ab initio/IGLO studies, and their role in cationic polymerization of cyclosiloxanes. J Am Chem Soc 117:8962–8966

Pfeifer H (1994) NMR of solid surfaces. In: Diehl P, Fluck E, Günther H, Kosfeld R, Seeing J (ed) NMR basic principles and progress, vol 33, Springer-Verlag, Berlin Heidelberg New York, pp31–90

Ramdas S, Klinowski J (1984) A simple correlation between isotropic ^{29}Si-NMR chemical shifts and T-O-T angles in zeolite frameworks. Nature 308:525–527

Rühlmann K, Scheim U, S.A. Evans J, Kelly JW, Bassindale AR (1988) Synthesis of siloxanes V. Oxygen-17 NMR spectroscopy. J Organomet Chem 340:19–21

Sauer J, Ugliengo P, Garrone E, Saunders VR (1994) Theoretical study of van der Waals complexes at surface sites in comparison with the experiment. Chem Rev 94:2095–2160

Schaefer HFI, Clemm RA, Harris FE (1968) Atomic hyperfine structure. I. Polarization wave functions for the ground states of B, C, N, O, and F. Phys Rev 176:49–58

Sherriff BL, Grundy HD (1988) Calculations of ^{29}Si MAS NMR chemical shift from silicate mineral structure. Nature 332: 819–822

Smith JV, Blackwell CS (1983) Nuclear magnetic resonance of silica polymorphs. Nature 303:223–225

Spearing DR, Farnan I, Stebbins JF (1992) Dynamics of the α-β phase transitions in quartz and cristobalite as observed by in-situ high temperature ^{29}Si and ^{17}O NMR. Phys Chem Minerals 19: 307–321

Stebbins JF (1995) Nuclear magnetic resonance spectroscopy of silicates and oxides in geochemistry and geophysics. In: Ahrens T J (ed) Mineral physics and crystallography, a handbook of physical constants. Washington, DC, American Geophysical Union, pp303–331

Stebbins JF, Kanzaki M (1991) Local structure and chemical shifts for six-coordinated silicon in high pressure mantle phases. Science 251:294–298

Sykes D, Kubicki JD, Farrar TC (1997) Molecular orbital calculation of ^{27}Al and ^{29}Si NMR parameters in Q^3 and Q^4 aluminosilicate molecules and implications for the interpretation of hydrous aluminosilicate glass NMR spectra. J Phys Chem 101:2715–2722

Timken HKC, Turner GL, Gilson J-P, Welsh LB, Oldfield E (1986a) Solid-state oxygen-17 nuclear magnetic resonance spectroscopic studies of zeolites and related systems. 1. J Am Chem Soc 108:7231–7235

Timken HKC, Janes N, Turner GL, Lambert SL, Welsh LB, Oldfield E (1986b) Solid-state oxygen-17 nuclear magnetic resonance spectroscopic studies of zeolites and related systems. 2. J Am Chem Soc 108:7236–7241

Timken HKC, Schramm SE, Kirkpatrick RJ, Oldfield E (1987) Solid-state oxygen-17 nuclear magnetic resonance spectroscopic studies of alkaline earth metasilicates. J Phys Chem 91:1054–1058

Tossell JA (1990) Calculation of NMR shieldings and other properties for three and five coordinate Si, three coordinate O and some siloxane and boroxol ring compounds. J Non-Cryst Solids 120:13–19

Tossell JA, Lazzeretti P (1988) Calculation of NMR parameters for bridging oxygens in H_3T-O-$T'H_3$ linkages (T, T'=Al, Si, P), for oxygen in SiH_3O^-, SiH_3OH and SiH_3OMg^+ and for bridging fluorine in $H_3SiFSiH_3^+$. Phys Chem Minerals 15:564–569

Tossell JA, Sághi-Szabó G (1997) Aluminosilicate and borosilicate single 4-rings: effects of counterions and water on structure, stability and spectra. Geochim Cosmochim Acta 61:1171–1179

Verhoeven J, Dymanus A, Bluyssen H (1969) Hyperfine structure of $HD^{17}O$ by beam-master spectroscopy. J Chem Phys 15:3330–3338

Walter TH, Turner GL, Oldfield E (1988) Oxygen-17 cross polarization NMR spectroscopy of inorganic solids. J Magn Reson 76:106–120

Xiao Y, Lasaga AC (1994) Ab initio quantum mechanical studies of the kinetics and mechanisms of silicate dissolution: $H^+(H_3O^+)$ catalysis. Geochim Cosmochim Acta 58:5379–5400

Xue X, Stebbins JF, Kanzaki M (1994) Correlations between ^{17}O NMR parameters and local structure around oxygen in high-pressure silicates: implications for the structure of silicate melts at high pressure. Am Mineral 79:31–42